

Quantification of Uncertainties for Evaluated Neutron-Induced Reactions on Actinides in the Fast Energy Range

P. Talou*, P.G. Young, and T. Kawano

*T-2, Nuclear Physics Group, Theoretical Division,
Los Alamos National Laboratory, Los Alamos, NM 87545, USA*

M. Rising

Department of Nuclear Engineering, University of New Mexico, Albuquerque, NM

M.B. Chadwick

X-CP, Los Alamos National Laboratory, Los Alamos, NM 87545, USA

(Received 12 July 2011; revised received 4 October 2011; accepted 7 October 2011)

Covariance matrix evaluations in the fast energy range were performed for a large number of actinides, either using low-fidelity techniques or more sophisticated methods that rely on both experimental data as well as model calculations. The latter covariance evaluations included in the ENDF/B-VII.1 library are discussed for each actinide separately.

Contents

I. INTRODUCTION

I. INTRODUCTION	1
II. METHODOLOGY	2
A. General Statements	2
B. Combining Model Calculations and Experimental Data	2
C. Types of Data Considered	2
D. Experimental Data Uncertainties	3
E. Codes Used	3
F. Present Limitations	3
III. RESULTS	4
A. ²³⁵ U	4
B. ²³⁸ U	6
C. ²³⁸ Pu	9
D. ²³⁹ Pu	13
E. ²⁴⁰ Pu	15
F. ²⁴¹ Pu	17
G. Other Actinide Evaluations	18
IV. SUMMARY AND OUTLOOK	19
Acknowledgments	20
References	20

At LANL, we started working on UQ for evaluated nuclear data about 6 years ago, just before the release of the

*Electronic address: talou@lanl.gov

ENDF/B-VII.0 library [2]. This VII.0 library constitutes a milestone in reliability, completeness and accuracy for many nuclear data. However, it contains close to zero covariance matrices, the solution of choice in the ENDF format to represent uncertainties associated with evaluated data.

The release of the ENDF/B-VII.1 library [3] is largely aimed at incorporating covariance matrices associated with a large number of nuclei and reactions. The present document describes selected UQ works performed at LANL for covariance evaluations of neutron-induced reactions on actinides in the fast energy range, above the resolved and unresolved resonance regions. For incident neutron energies ranging from thermal to the unresolved resonance region, ORNL has led those efforts and provided a relatively large number of covariance matrix evaluations as well (see L. Leal *et al.* [4]).

In the following, we focus on UQ for neutron-induced reactions on actinides in the fast energy range. The methodology, types of data considered as well as the nuclear reaction codes and statistical codes used in this work are described in the next section. It is followed by a detailed discussion of the results obtained for $n+^{235,238}\text{U}$ and $n+^{238-241}\text{Pu}$. Other UQ results were obtained for $n+^{233}\text{U}$ and $n+^{241}\text{Am}$ and, although not discussed in the present paper, have been included in the ENDF/B-VII.1 library.

Note that various UQ methodologies in nuclear data evaluations in the fast energy range have been the focus of the OECD WPEC Subgroup-24. Its report [5] provides a comprehensive view of those different approaches, including the one used in the present work.

II. METHODOLOGY

A. General Statements

It is important to recognize that an uncertainty is not a physical quantity, but instead a measure of our knowledge on this physical quantity. An important consequence of this seemingly simple statement is that there is no right or wrong uncertainty- except in the case of an erroneous analysis on the part of the evaluator of course, and that comparisons between evaluated covariance matrices are rather meaningless without specifying which information have been included in the evaluation. For instance, a model-based evaluation will lead to very different correlation coefficients than if the analysis is based uniquely on experimental data.

In the best case scenario, the quantification of uncertainties associated with an evaluated nuclear data should follow precisely the methods that have been used in the evaluation, and identify all sources of uncertainties therein. In the present work, this situation rarely occurred due to the complexity and variety of tools used in the evaluation process. This remark should serve as an important caveat in the discussion below, and emphasizes

that much work remains to be done to fully integrate the evaluation and UQ processes in one single phase of “data assimilation”.

B. Combining Model Calculations and Experimental Data

The uncertainty quantification (UQ) methodology used for actinide evaluations in the fast energy range for ENDF/B-VII.1 represents an attempt to combine all sources of uncertainties that pertain to the evaluation itself. Since the evaluation results from nuclear model calculations as well as a study of differential experimental data, the uncertainty quantification reflects both sources of uncertainties in the model parameters and the experimental values. Bayes’ theorem [6] is used throughout our UQ work to perform this combination, and can be summarized with the following equations:

$$\begin{aligned} \mathbf{m}_1 &= \mathbf{m}_0 + \mathbf{P}\mathbf{C}^t\mathbf{V}^{-1}(\mathbf{y} - f(\mathbf{m}_0)) \\ &= \mathbf{m}_0 + \mathbf{X}\mathbf{C}^t(\mathbf{C}\mathbf{X}\mathbf{C}^t + \mathbf{V})^{-1}(\mathbf{y} - f(\mathbf{m}_0)), \end{aligned} \quad (1)$$

$$\begin{aligned} \mathbf{P} &= (\mathbf{X}^{-1} + \mathbf{C}^t\mathbf{V}^{-1}\mathbf{C})^{-1} \\ &= \mathbf{X} - \mathbf{X}\mathbf{C}^t(\mathbf{C}\mathbf{X}\mathbf{C}^t + \mathbf{V})^{-1}\mathbf{C}\mathbf{X}. \end{aligned} \quad (2)$$

Here, \mathbf{m}_0 represents the vector of *prior* model parameters, and \mathbf{m}_1 is the vector of *posterior* model parameters. The quantity $f(\mathbf{m}_0)$ is the calculated quantity using *prior* parameter values. \mathbf{y} is the experimental data, \mathbf{X} and \mathbf{P} are the *prior* and *posterior* model parameter covariance matrices, respectively. Finally, \mathbf{V} represents the experimental covariance matrix, and \mathbf{C} the sensitivity matrix whose elements are given by

$$C_{ij} = \frac{\partial f_i(\mathbf{m})}{\partial m^j}. \quad (3)$$

This equation assumes that the response of the quantity y_i to a change in model parameter m^j is linear in the first-order approximation.

Finally, covariance matrices for cross sections, spectra, etc, are obtained as

$$\mathbf{F} = \mathbf{C}\mathbf{P}\mathbf{C}^t. \quad (4)$$

Prior model parameter uncertainties are often considered uncorrelated, and correlations are brought in through Bayes’ equations 1 and 2. Those correlations stem from the physical models used in the theoretical calculations, as well as from systematic uncertainties associated with the observed data.

C. Types of Data Considered

In the present work, all major reaction cross sections are considered- total, capture, fission, elastic, total inelastic, and (n,xn), but neither angular distribution nor discrete inelastic reaction uncertainties were considered. However, in some cases, i.e., $n+^{238-240}\text{Pu}$ and

$n+^{235,238}\text{U}$, the prompt fission neutron spectrum covariance matrix was evaluated at 0.5 MeV incident neutron energy, following an approach similar to the one developed for cross section uncertainties [7]. Also the average prompt fission neutron multiplicity $\bar{\nu}_p(E_{inc})$ was usually evaluated through a statistical analysis of experimental data, when available.

D. Experimental Data Uncertainties

Uncertainties associated with data measurements come in a variety of flavors but fall squarely in two distinct categories: (i) statistical, i.e., the uncertainties can be reduced to infinitely small values if the same experiment is repeated for ever; (ii) systematic, i.e., those uncertainties do not disappear by simply repeating the experiment and reflect the limit of our knowledge on various parameters of the experiment (target composition, flux homogeneity, detector efficiency, etc). Statistical uncertainties have no correlation from one data point to another, contrary to systematic uncertainties which can lead to very strong correlations between measured points as well as between experiments.

In the present work, both statistical and systematic uncertainties are taken into account. However, serious limitations exist in the derivation of experimental covariance matrices when little to no information is known on the experimental conditions. Even in the case of relatively well described experimental uncertainties, more evaluation efforts need to be done to better represent the experimental covariance matrices used in this work.

E. Codes Used

A set of codes is common to all evaluations and uncertainty quantifications reported here. Coupled-channel calculations were performed with the ECIS code [8], in one of its recent incarnations from 1996, 2003, or 2006. The GNASH code [9] was used for most nuclear reaction calculations in the statistical Hauser-Feshbach formalism. The COH code [10] was also used at times, in particular to better compute the capture cross-section at low energy. The PFNS code [11] was used to compute prompt fission neutron spectra using the Los Alamos or Madland-Nix model [12]. Sensitivity calculations were performed and analyzed using a suite of Perl scripts, while the KALMAN code [13] was used to perform the Bayesian inference computations. Finally, covariance matrices were transformed in ENDF format and processed by the NJOY code [14].

F. Present Limitations

At present, there are several limitations that prevent those covariance evaluations to be fully representative of the data evaluation themselves.

In the first place, no model deficiency is considered, i.e., all sources of uncertainties coming from model calculations stem for the uncertainty in the model parameters, making the assumption that the models are perfect, at least in the domain of isotopes and energy ranges where they are applied. An exception was made in the case of the $n+^{239}\text{Pu}$ prompt fission neutron spectrum covariance matrix for which a model deficiency component was added following an *ad hoc* prescription. Obviously, model deficiencies are intrinsically difficult to assess, but some attempts are being made to address this issue [15].

The total elastic cross section uncertainties are derived from uncertainties evaluated in the other channels, with constraints from the total cross section evaluated uncertainties. The NJOY code actually infers the cross-correlation coefficients from such a constraint, as they are not given directly in the evaluated files. Instead they are given as so-called “derived redundant cross sections” as a NC-type sub-subsection with LTY=0. The inferred cross-section covariance matrix is obtained following the “derivation relation” as explained in the NJOY manual under the ERRORR section, Eq. 17, X-7 [14].

Another limitation is of more general nature: the UQ process does not strictly follow the evaluation process. The reasons are manifold but two are most prominent: (i) our UQ tools are not yet fully integrated into the evaluation toolkit; (ii) the UQ process does not fully grasp the input information that go into an evaluated data file, and is therefore not exactly representative of the evaluation itself. For instance, feedback from “clean” integral benchmarks, such as GODIVA and JEZEBEL fast critical assemblies, are often used to test evaluated files for important materials such as ^{235}U and ^{239}Pu . Slight adjustments on individual evaluated cross-sections, neutron multiplicities and spectra are often carried out so that C/E values for integral quantities such as the multiplicative factor k_{eff} remain very close to unity. These *ad-hoc* adjustments are never included in any type of UQ process, but evaluated files are adjusted nonetheless.

While the evaluation of nuclear data for actinides can clearly be separated in a resolved resonance range at the lowest energies and a fast energy range, using different representations of the nuclear reaction theories that pertain to each energy range, the intermediate unresolved range connects both lower and higher energies where various physics models meet. A more comprehensive evaluation and UQ approach of the unresolved resonance range should bring correlations across the full energy range from thermal up to a few tens of MeV. While those correlations are expected to be small, they should appear in the URR covariance matrix, if such correlations are taken into consideration during the evaluation process. At present, we did not include any such correlation.

There is no doubt that all those limitations can be removed over time by developing improved *data assimilation* packages that can clearly identify all sources of uncertainty and correlation.

III. RESULTS

The uncertainty quantification work discussed here started with an evaluation effort for neutron-induced reactions on the three major isotopes ^{235}U , ^{238}U and ^{239}Pu and partial results have already been reported in Ref. [16]. Similar efforts were pursued later on for other U and Pu isotopes, as well as for ^{241}Am . In this Section, we discuss the results obtained for each nucleus.

A. ^{235}U

As mentioned earlier, covariance evaluations for $n+^{235}\text{U}$ were performed prior to, but associated with the release of the ENDF/B-VII.0 library. We extend here some of the results already reported at the ND2007 Conference [16].

Coupled-channel calculations were performed using the ECIS code and the optical potential developed by P.G. Young [17], which is indexed number 3 in the RIPL-3 database [18]. The total, reaction and shape elastic cross sections were obtained, and model parameter sensitivity calculations were performed by varying the following optical model parameters: the depth, radius and diffuseness of the real volume, imaginary volume, and real surface terms, as well as the (β_2, β_4) deformation parameters. The KALMAN code was then used to combine model parameter sensitivity calculations with experimental data uncertainties.

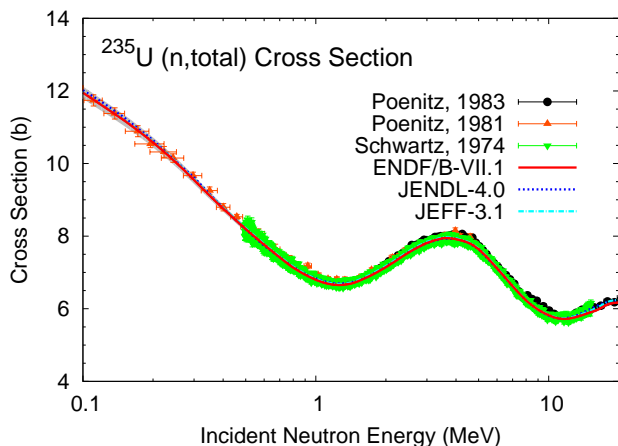


FIG. 1: The ENDF/B-VII.1 evaluated ^{235}U (n,total) cross-section reaction is compared to a subset of all experimental data and to other evaluations. The 1σ error band is also shown as a gray band.

The calculated (n,total) cross-section is shown in Fig. 1, with a one-sigma band shown in gray, barely visible because of the small evaluated standard deviations. The evaluated standard deviations can be better seen in Fig. 10. The evaluated covariance matrix for the total cross section is then used to constrain all other partial

reaction channels, through the NJOY code.

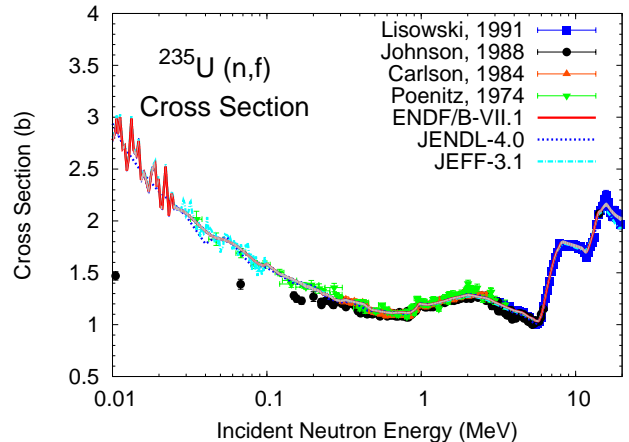


FIG. 2: The ^{235}U (n,f) cross section in ENDF/B-VII.1 (= VII.0) was taken directly from the cross section standards analysis by Carlson *et al.* [19]. A subset of all experimental data sets is also shown, and comparisons are made with other current evaluated libraries.

The neutron-induced fission cross section of ^{235}U was evaluated recently by the IAEA Standards Group [19], and the ENDF/B-VII.0 evaluation incorporate their findings without modification, including the associated covariance matrix for this reaction. The ^{235}U (n,f) cross section is shown in Fig. 2 with a subset of experimental data and evaluated libraries. Overall, the evaluated standard deviations are very small, less than 1% (see Fig. 10). The correlation matrix is shown in Fig. 3. The off-diagonal elements are all positive and very small due to the large number of experimental data sets incorporated in the evaluation.

The estimation of uncertainties associated with the neutron-induced fission cross-section of ^{235}U is of major importance as most other actinide fission cross-section uncertainties are driven by it. Indeed, a great number of fission cross-section measurements are performed in *ratio* to the ^{235}U (n,f) cross-section, and uncertainties for other actinides are propagated proportionally to those in ^{235}U . While the evaluation by the IAEA Standards Group [19] is the result of major efforts from experts in the domain, unrecognized correlations between experiments can certainly lead to an underestimation of the final uncertainties. The development of a time-projection chamber (TPC) for sub-percent fission cross-section measurements [add TPC reference] represents an important effort to evaluate this cross-section in a very different approach than what has been done in the past. In this sense, the results of a TPC measurement would be mostly uncorrelated to past data sets, and would represent a strong test for the current evaluation.

Direct measurements of the capture cross section of fissile nuclei are challenging and subject to large errors due to the difficulty in distinguishing capture from fission events. More commonly the ratio $\alpha = \sigma_c/\sigma_f$ of the

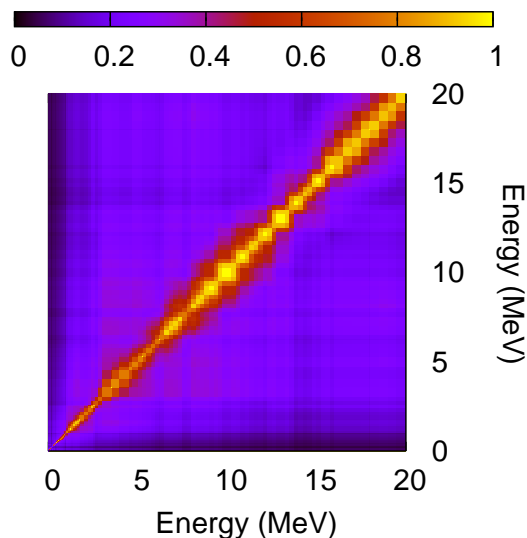


FIG. 3: Correlation matrix for the neutron-induced fission cross section on ^{235}U . It was evaluated by Pronyaev *et al.* as part of the cross section standards evaluation [19].

capture-to-fission cross sections is measured, as shown in Fig. 4 with a subset of all experimental data available. Note that most data reported in the EXFOR database have already been converted to absolute cross-sections, while measured ratio data have not been kept. The reported experimental data are rather consistent with each other, albeit exhibiting large uncertainties.

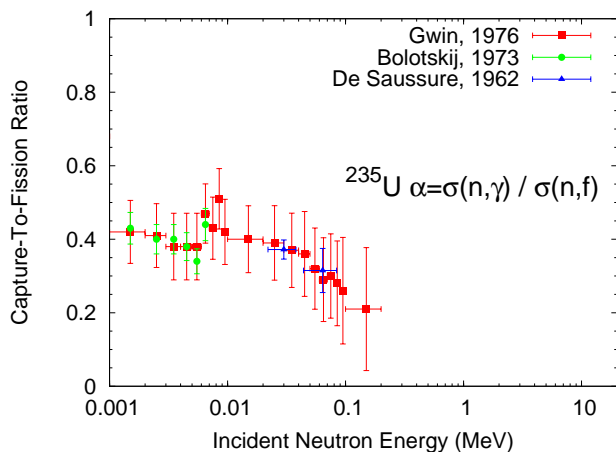


FIG. 4: Experimental data on the capture-to-fission cross-sections ratio for the ^{235}U (n,f) reaction.

The ENDF/B-VII.1 evaluated ^{235}U neutron-induced capture cross-section is shown in Fig. 5 with experimental data and other evaluated libraries. In this case, the relative agreement between evaluations is not a good indicator of how well this cross-section is known, and relatively large uncertainties remain in the 10–200 keV region (about 30%). The correlation matrix for the capture

cross-section evaluated uncertainties is shown in Fig. 6, and exhibits very large off-diagonal elements.

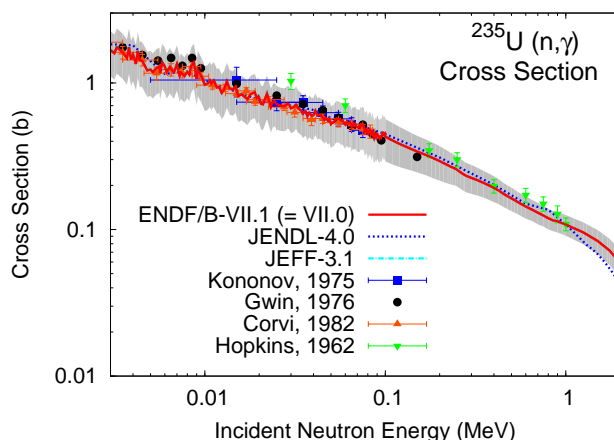


FIG. 5: The ENDF/B-VII.1/0 evaluated capture cross-section for the $n+^{235}\text{U}$ reaction is compared with experimental data and other evaluated libraries. The JEFF-3.1 library is identical to the ENDF/B evaluation.

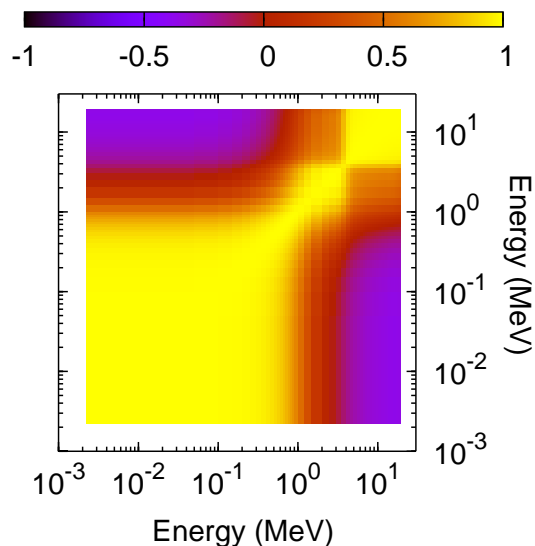


FIG. 6: Correlation matrix for the capture cross section of $n+^{235}\text{U}$.

The ENDF/B-VII.1 (= VII.0) evaluated ^{235}U ($n,2n$) and ($n,3n$) cross sections are shown in Figs. 7 and 8 in comparison with other current evaluations and experimental data sets. Most evaluations agree fairly well with the experimental data by Frehaut [20] and Mather [21], except with the data point at 14.1 MeV that lies well below the evaluated results. This low-value is partly compensated by a higher value for the ($n,3n$) cross section at 14.1 MeV, which is higher than all evaluations, and

outside the uncertainty band evaluated for the ENDF/B-VII.1 values.

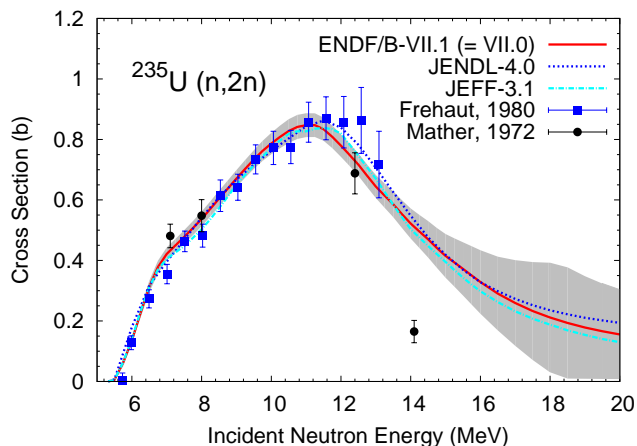


FIG. 7: The ENDF/B-VII.1 (= VII.0) evaluated $^{235}\text{U}(n,2n)$ cross-section is compared with experimental data and other evaluated libraries.

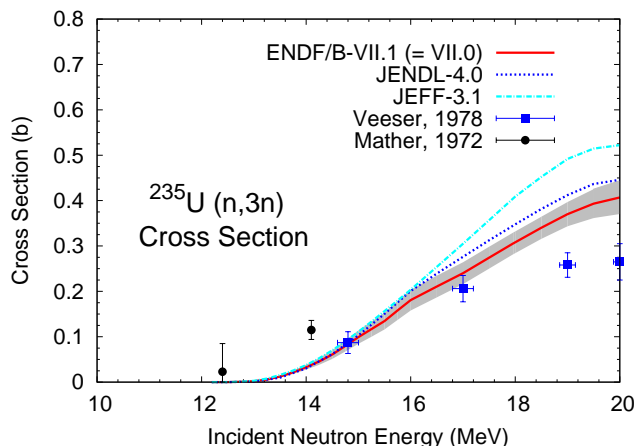


FIG. 8: The ENDF/B-VII.1 (= VII.0) evaluated $^{235}\text{U}(n,3n)$ cross-section is compared with experimental data and other evaluated libraries.

The total inelastic cross section for $n+^{235}\text{U}$ reaction is shown in Fig. 9 with experimental data sets and other evaluations. It was calculated by summing all the discrete and continuum contributions. The ENDF/B-VII.1 (= VII.0) result is in agreement, within one-sigma, with the JENDL-4.0 and JEFF-3.1 evaluations, and is in fair agreement with the experimental data, except from threshold up to 2 MeV where the evaluation lies higher than most data points.

A summary plot of the standard deviations evaluated for all the major reaction cross sections on $n+^{235}\text{U}$ is given in Fig. 10.

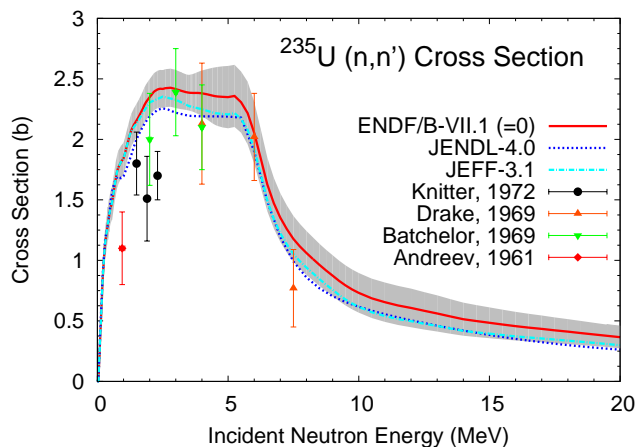


FIG. 9: The ENDF/B-VII.1/0 evaluated $^{235}\text{U}(n,n')$ total inelastic cross-section is compared with experimental data and other evaluated libraries.

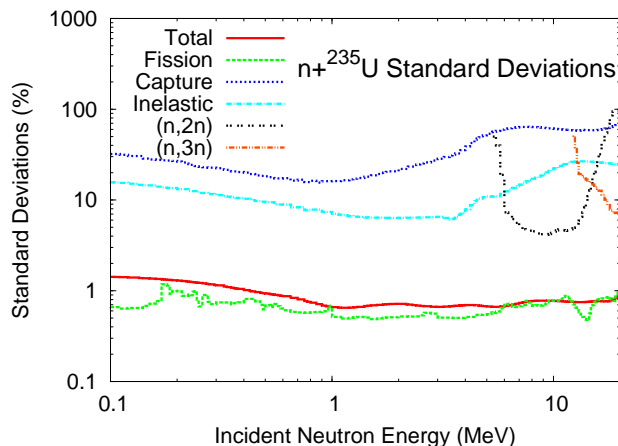


FIG. 10: The relative standard deviations evaluated for the major reaction cross sections for $n+^{235}\text{U}$. The label “Standard Deviations” in this figure and similar ones later is really a shortcut for “relative standard deviations”, expressed in percent.

B. ^{238}U

As was the case for $n+^{235}\text{U}$ and $n+^{239}\text{Pu}$ reactions, the uncertainty quantification work for $n+^{238}\text{U}$ reaction cross sections was performed prior to the ENDF/B-VII.0 library release, but the results were not incorporated in the library at that time. Some results are reported and discussed here.

The evaluated $^{238}\text{U}(n,\text{total})$ cross-section and its one-sigma uncertainty band is shown in Fig. 11, and compared to experimental data sets and other evaluations. The evaluated uncertainties are larger than those estimated for $^{235}\text{U}(n,\text{total})$ cross sections but remain at less than 5% for all energies (see Fig. 19).

The ENDF/B-VII.1 evaluation for the ^{238}U neutron-

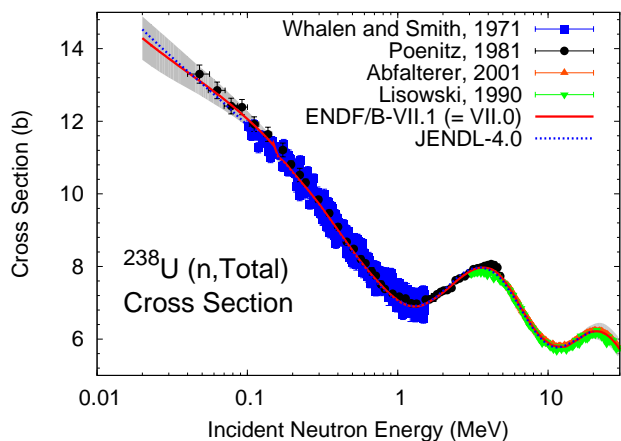


FIG. 11: $^{238}\text{U}+n$ total cross section, with its evaluated 1σ uncertainty band, compared to experimental data sets and other evaluations.

induced fission cross section, shown in Fig. 12 is unchanged from VII.0, which, from 20 keV to 1.0 MeV is the same as the ENDF/B-VI.8 evaluation. It relies entirely on experimental data sets, either on the unresolved resonance parameters of Fröhner and Poenitz [22, 23] or on the ENDF/B-VII standards analysis of Pronyaev *et al.* [19]. The different major evaluated libraries agree reasonably well with each other below 20 MeV, and with the standard deviations evaluated for ENDF/B-VII.1, which is typically around 1%. The fission cross section correlation matrix is shown in Fig. 13 and is nearly diagonal, a result from the relatively large body of experimental data with very little assumed correlations between them.

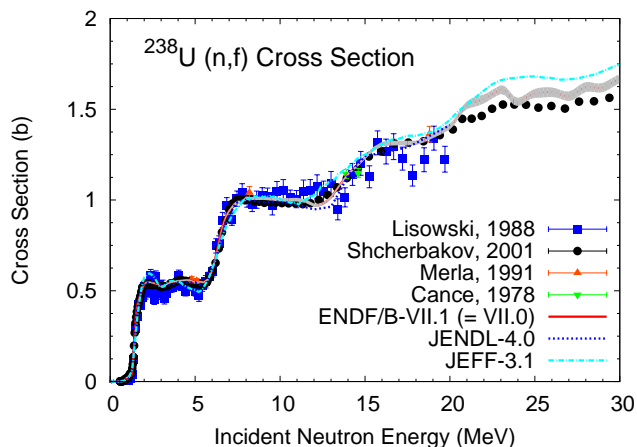


FIG. 12: Neutron-induced fission cross-section of ^{238}U compared to a subset of experimental data, and other evaluated libraries.

Similar to fission, the evaluated $^{238}\text{U}(n,\gamma)$ cross section is based on experimental data at most energies. It is shown in Fig. 14 and is compared to various evaluations and experimental data sets. From 149 keV to 2.2

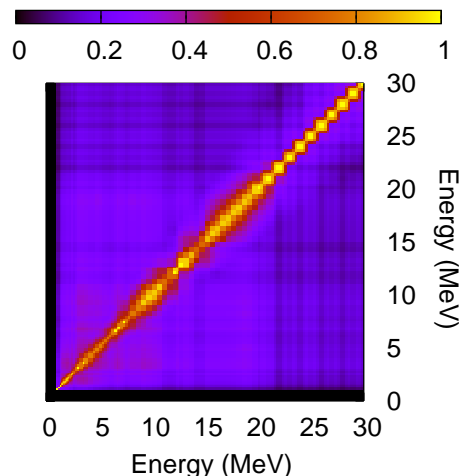


FIG. 13: ^{238}U fission cross-section correlation matrix.

MeV, the evaluation closely follows results from the standards analysis by Carlson *et al.* [19]. Above 2.2 MeV, the evaluation is based on the JENDL-3.0 evaluation, with a smooth extrapolation from 20 to 30 MeV. The evaluated $^{238}\text{U}(n,\gamma)$ capture cross section is lower than most measurements below 1 MeV, as discussed by the standards evaluators. The same conclusion was reached by the NEA WPEC Subgroup-4 [24]. Large discrepancies occur between different measurements in the 8 to 14 MeV region, where the evaluation follows the data by Drake *et al.* [25] and McDaniels *et al.* [26].

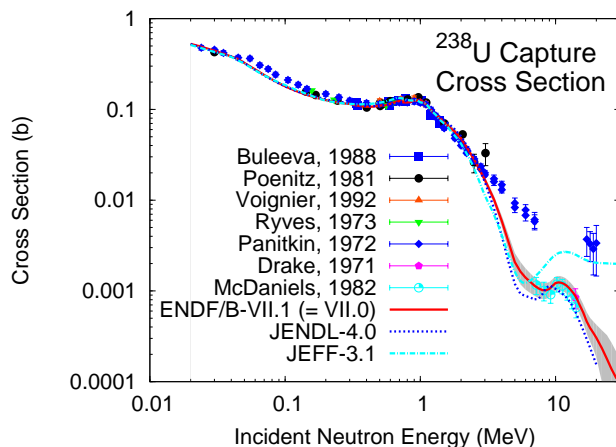


FIG. 14: ^{238}U capture cross-section compared to experimental data and other evaluated libraries.

The uncertainties for the $^{238}\text{U}(n,\gamma)$ cross section were taken from the standards evaluation work by Pronyaev *et al.* [19], and are typically lower than 2% below 1 MeV. The discrepancies between data sets above 8 MeV are clearly not accounted for in our UQ results, but are instead constrained by the theoretical model parameter uncertainties and the experimental uncertainties of Drake *et*

al. and McDaniel *et al.*

The total inelastic cross section $^{238}\text{U}(n,n')$ is shown in Fig. 15 and compared with other evaluations and experimental data. While the evaluations agree reasonably well with each other near the threshold, relatively large discrepancies appear at higher energies. At 14 MeV however, they again agree with each other, while most experimental points lie lower, probably due to the low-energy cutoff of the detectors used to measure the neutron spectra.

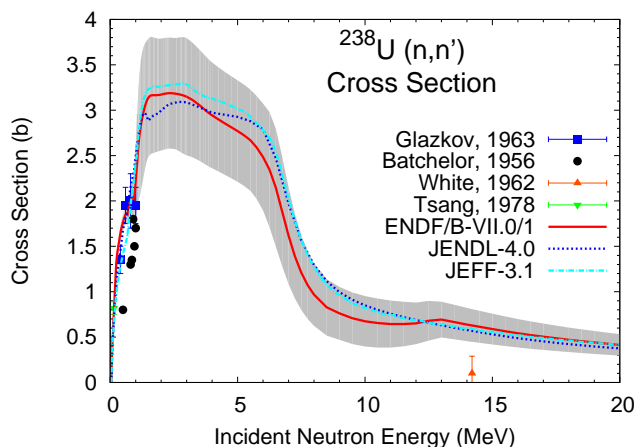


FIG. 15: $^{238}\text{U}(n,n')$ total inelastic cross-section.

A relatively large body of experimental data exist for the $^{238}\text{U}(n,2n)$ reaction cross section as shown in Fig. 16, which explains the relatively small uncertainties evaluated for this particular reaction, mostly below 10% except very close to threshold (see Fig. 19).

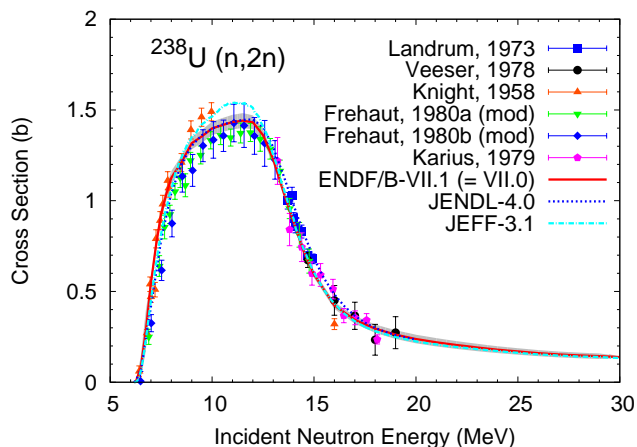


FIG. 16: Evaluated and experimental cross sections for the $^{238}\text{U}(n,2n)$ reaction from threshold to 20 MeV.

The $^{238}\text{U}(n,3n)$ cross section evaluation is based on GNASH calculations, slightly modified to agree with experiment and renormalized above 20 MeV. The uncertainties are relatively small, due to accurate experimental

data by Frehaut *et al.* [20] and Veerer and Arthur [27].

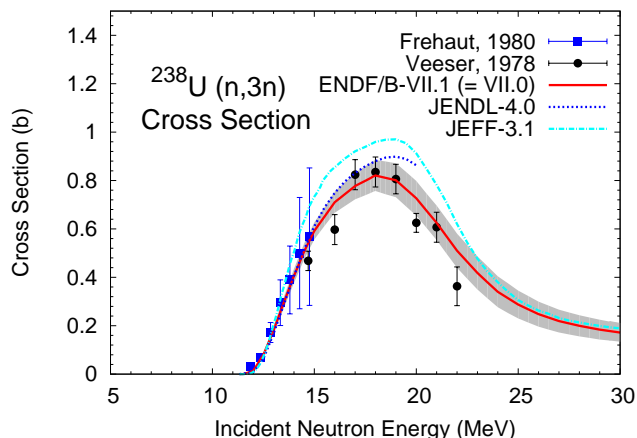


FIG. 17: $^{238}\text{U}(n,3n)$ cross-section compared to experimental data by Frehaut *et al.* [20] and Veerer and Arthur [27], and other evaluations.

The ENDF/B-VII.0 evaluation of the average prompt fission neutron multiplicity $\bar{\nu}_p$ for $n+^{238}\text{U}$ is taken from VI.8, which in turn is based on an evaluation by Frehaut [28] using the already extensive experimental database available at that time. More recent data by Taieb *et al.* [29] and Boykov *et al.* [30] seem to indicate smaller $\bar{\nu}_p$ values for incident energies above 5 MeV. However, it is likely that the uncertainties associated with those new data points are under-estimated due to the particular experimental setup used. The uncertainties evaluated by Frehaut, and therefore in ENDF/B-VII.1, do not reflect these discrepancies.

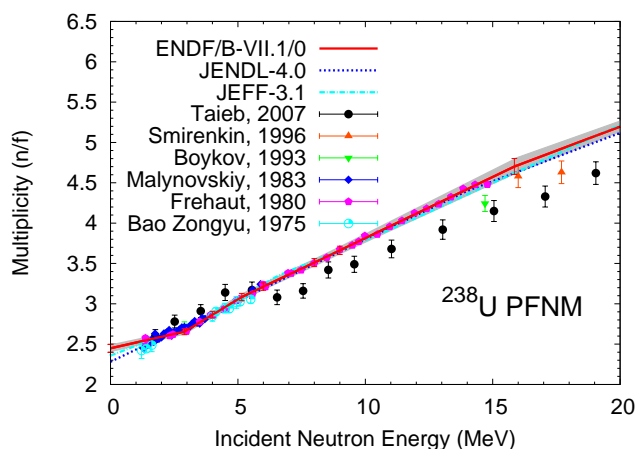


FIG. 18: Prompt fission neutron multiplicity evaluated for the $^{238}\text{U}(n,f)$ reaction, and compared to a subset of experimental data and other evaluated libraries.

A summary plot of the major cross-section standard deviations for $n+^{238}\text{U}$ reactions in the fast energy range is shown in Fig. 19.

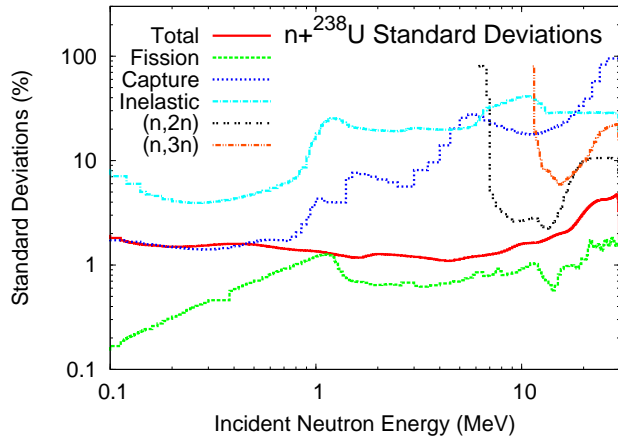


FIG. 19: Cross-section standard deviations evaluated for neutron-induced reactions on ^{238}U .

No uncertainty quantification has been performed yet for the evaluated prompt fission neutron spectra.

C. ^{238}Pu

A new evaluation of $n+^{238}\text{Pu}$ was performed for the ENDF/B-VII.1 library. Experimental data are scarce for neutron-induced reactions on ^{238}Pu except in the case of fission, as summarized in Table I. There is only one measurement for the total cross section by T.E. Young *et al.* [45] in the resolved and unresolved range, stopping near 10 keV incident energy, and only one capture cross section measurement by Silbert and Berreth [31].

Since no data exist for the (n,total) cross-section (the data by T.E.Young stop in the URR), the UQ results are based entirely on ECIS model sensitivity calculations. The optical potential developed by Soukhovitskii *et al.* [48] was used in an ECIS coupled-channel calculation, and various optical potential parameters were varied to obtain the relative sensitivity coefficients $S_p = \partial\sigma(n,\text{tot})/\partial p$. The most important parameters turned out to be the parameters for the real volume potential $\{v, r_v, a_v\}$ as well as the quadrupole deformation β_2 . Figure 20 shows the relative sensitivity coefficients obtained for those parameters as a function of the incident neutron energy.

Since no experimental data exist beyond about 6 keV (our transition energy from the resolved resonance range), the evaluated uncertainties are the direct consequence of uncertainties assumed in the model parameters. We have assumed a 2% uncertainty on all parameter values, leading to the results shown in Fig. 21.

The COH code [10] was used to calculate the capture cross-section. Only one experimental data set exists for this reaction, and was obtained by Silbert and Berreth [31]. The experimental points extend up to about 200 keV, but the reported uncertainties are very

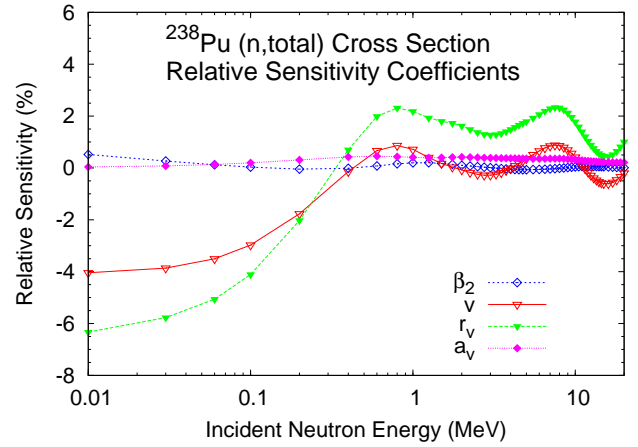


FIG. 20: Relative sensitivity coefficients for the total cross section of $n+^{238}\text{Pu}$. The most important parameters in the coupled-channel calculations are the quadrupole deformation parameter β_2 , and the parameters for the real volume potential (v, r_v, a_v).

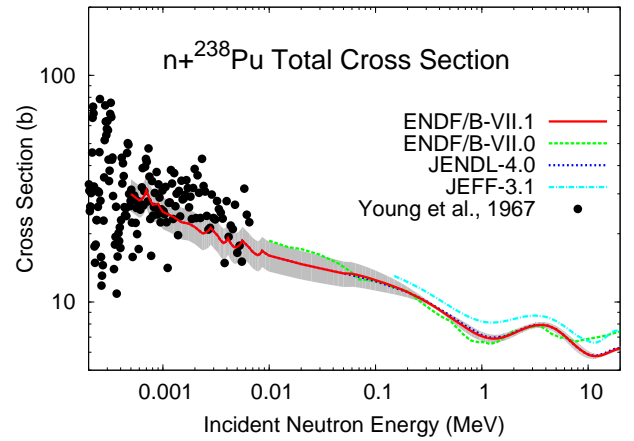


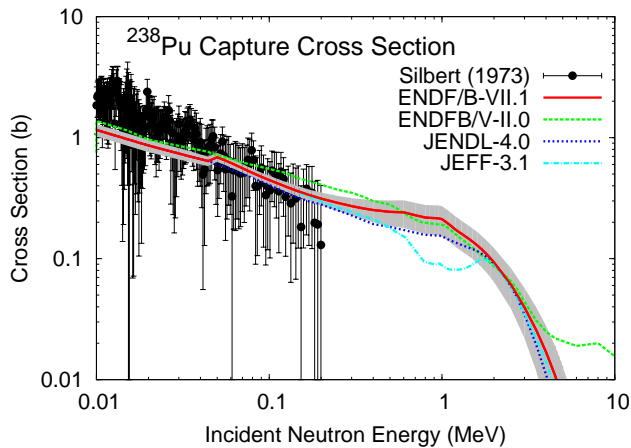
FIG. 21: The evaluated ^{238}Pu (n,total) cross section is compared to other current evaluated libraries. The one-sigma uncertainty band was obtained by assuming 2% uncertainties in the optical model potential parameters (v, r_v, a_v, β_2).

large there ($\sim 50\text{-}200\%$). A comparison of the calculated cross section, experimental data, and evaluated libraries is shown in Fig. 22.

Fission cross-section uncertainties were evaluated using a generalized least-square fit of the experimental data sets. The result is shown in Fig. 23. There are quite a few experimental measurements of the fission cross section in the unresolved resonance range and the fast energy regime. One discrepant data set (by Butler *et al.*, 1963) was significantly downgraded in the evaluation by amplifying the reported uncertainties. There is a specific energy region, just above 10 MeV, where data are lacking. In this case, our Bayesian statistical analysis, performed with the GLUCS code, provides unrealistically large uncertainties. We modified the prior information used in

TABLE I: The experimental database for neutron-induced reactions on ^{238}Pu which has been used in the present work.

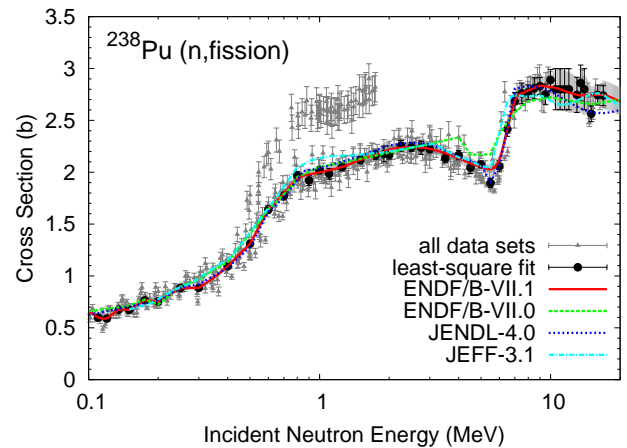
Reaction	EXFOR Entry	First Author	Year	Reference
Total	12484-008	T.E.Young	1967	(J,NSE,30,355,1967)
Capture	10032-005	M.G.Silbert	1973	(J,NSE,52,176,1973)
Fission	41303-015,17	B.I.Fursov	1997	(C,97TRIST,1,488,199705)
	12991-004	B.Alam	1988	(J,NSE,99,267,198807)
	40673-003	B.M.Aleksandrov	1983	(J,YK,1/50,3,8303)
	21828-002	C.Budtz-Jørgensen	1982	(C,82ANTWER,,206,8209)
	10032-005	M.G.Silbert	1973	(J,NSE,52,176,1973)
	10061-002	D.M.Drake	1970	(R,LA-4420,101,197004)
	40012-008	E.F.Fomushkin	1969	(J,YF,10,(5),917,6911)
	40253-002	S.B.Ermagambetov	1968	(J,AE,25,(6),527,6812)
	12490-002	D.M.Barton	1967	(J,PR,162,1070,67)
	40779-002	E.F.Fomushkin	1967	(J,YF,5,(5),966,6705)
	12480-002	D.K.Butler	1963	(J,BAP,8,369(RA7), 6304)

FIG. 22: The calculated radiative capture of $n+^{238}\text{Pu}$ is compared to the experimental data of Silbert and Berreth [31], and with the ENDF/B-VII.0, JEFF-3.1, and JENDL-4.0 evaluations.

GLUCS to obtain more realistic final uncertainties in this energy domain, where no large fluctuation of the fission cross-section are expected.

Figure 24 shows the ENDF/B-VII.1 evaluation with recent experimental data obtained by Ressler *et al.* [35] at LLNL using the surrogate technique, and with preliminary data by Granier *et al.* [36]. The LLNL surrogate data are in good agreement with the evaluation in the 7-12 MeV range but lie higher elsewhere. The data by Granier *et al.* are consistently lower than the evaluation above 7 MeV incident energy. Those discrepancies need to be resolved to ensure consistency with the present ENDF/B-VII.1 evaluation.

Because our GLUCS statistical analysis does not consider cross-correlations between different experimental data sets, the evaluated correlation matrix shows a narrow band around the diagonal only, while far off-diagonal coefficients are washed away (see Fig. 25). The final re-

FIG. 23: Evaluated neutron-induced fission cross-section on ^{238}Pu compared to experimental data. The least-square result is shown as black solid circles.

sult was obtained by scaling both the diagonal elements (standard deviations) and the off-diagonal elements of the covariance matrix obtained with GLUCS.

Other (n,xn) cross section uncertainties were evaluated using GNASH model parameter sensitivity calculations and the KALMAN code. In most cases, the final uncertainties were scaled up by the χ^2/N between experiments and model calculations to compensate for the lack of proper correlation matrices between experimental data sets.

A summary of the standard deviations evaluated for all major reaction channels is shown in Fig. 26.

Uncertainties on the prompt fission neutron spectrum (PFNS) and multiplicity (PFNM) for $n+^{238}\text{Pu}$, evaluated using the Los Alamos model [12], were also quantified. The systematics developed by Tudora and Vladuca on the model input parameters [32] were used as prior parameters in our analysis. Very little experimental data exist on the neutron multiplicity- only two values

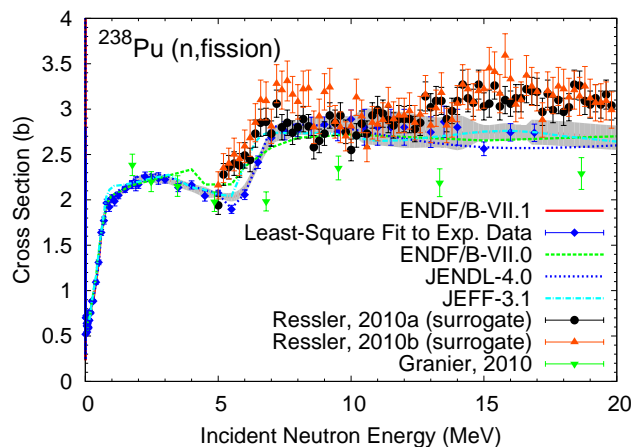


FIG. 24: Same as in Fig. 23 but including results from surrogate reactions. Those indirect experimental data sets were not included in our statistical analysis.

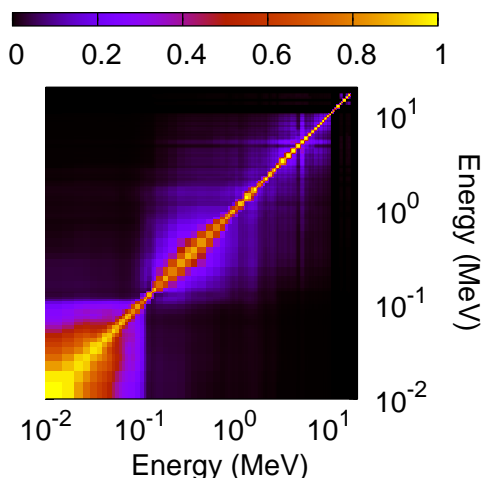


FIG. 25: Correlation matrix evaluated for the ^{238}Pu (n,fission) cross section.

reported in the EXFOR database at thermal energy, and none on the experimental spectrum, except for one value on the average neutron outgoing energy. Because of this, the evaluated spectrum uncertainties are due entirely to the uncertainties placed on the Los Alamos model input parameters.

The spectrum was evaluated for 21 incident energies from thermal up to 20 MeV, on the same energy grid as for ^{239}Pu . This is to be compared with the ENDF/B-VII.0 file for ^{238}Pu , which contains only one spectrum—a Maxwellian at temperature 1.33 MeV, for all incident energies. Results for 0.5 and 20.0 MeV incident neutron energies are shown in Figs. 27 and 28. For energies higher than about 5 MeV, multi-chance fission is included, using the n^{th} -chance fission probabilities calculated with

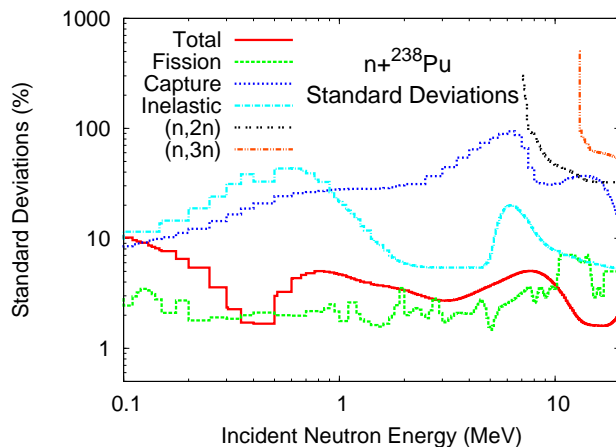


FIG. 26: Standard deviations evaluated for all major reaction channels for $n+^{238}\text{Pu}$.

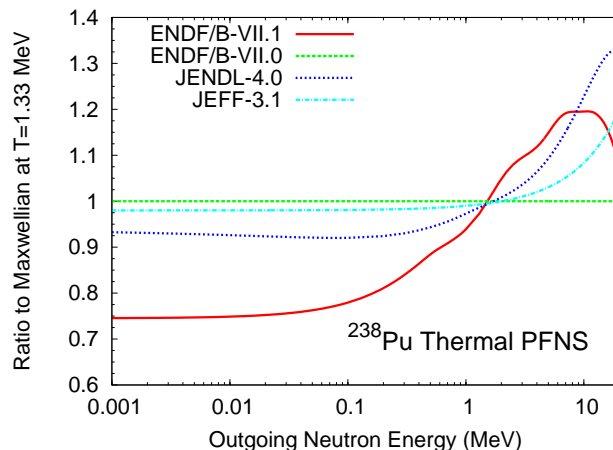


FIG. 27: Prompt fission neutron spectrum evaluated for the neutron-induced fission reaction of ^{238}Pu with thermal energy incident neutrons, and shown as a ratio to a Maxwellian at temperature $T=1.33$ MeV.

the GNASH code. The inclusion of multi-chance fission explains the drastic change observed for the 20.0 MeV PFNS compared to the existing ENDF/B-VII.0 result, which is given by the same Maxwellian as for low incident neutron energies. Figure 28 clearly displays the discrepancies observed between the ENDF/B-VII.0 file and the new result, which follows somewhat other current libraries.

To quantify uncertainties, we have followed the same approach as for cross sections, as described in more detail in Ref. [7]. The average energy release, total kinetic energy, level density, separation energy, binding energy and total gamma ray energy parameters in the Los Alamos model were assumed to be random variables. By placing an 8% uncertainty on the energy release, a 5% uncertainty on the total kinetic energy, and a 10% uncertainty on each of the level density, separation energy, binding en-

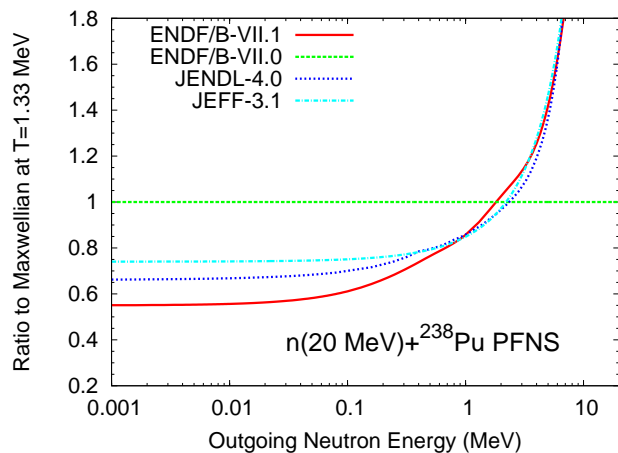
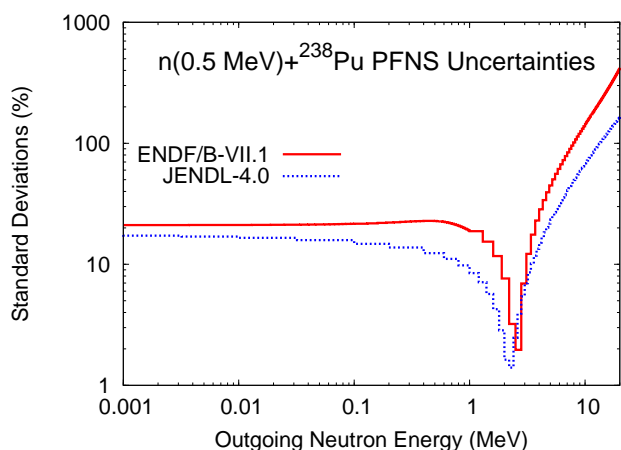


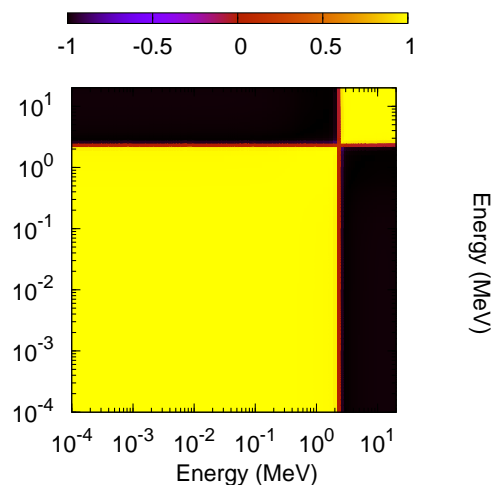
FIG. 28: Same as Fig. 27 but for 20 MeV incident neutrons.

ergy and total gamma ray energy, the posterior spectrum uncertainty and covariance matrix were inferred using the KALMAN code (Bayesian statistics).

FIG. 29: Standard deviations evaluated for the $n(0.5 \text{ MeV})+^{238}\text{Pu}$ prompt fission neutron spectrum, and compared to the JENDL-4.0 evaluated values.

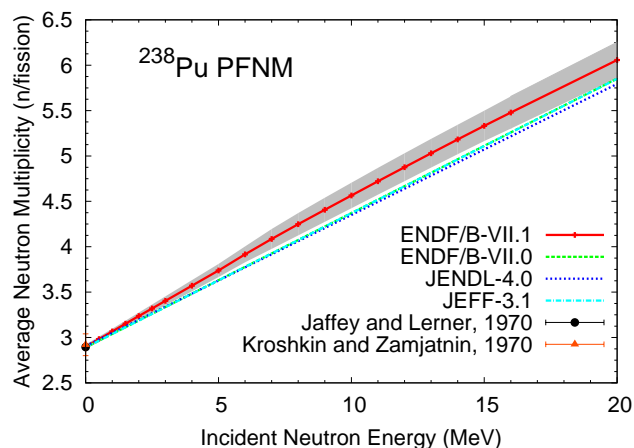
In Fig. 29 the standard deviation is shown as a percentage of the fission spectrum and in Fig. 30 the correlation matrix is shown. Once again, because of the lack of experimental data for this actinide, the correlation matrix and standard deviations of the fission spectrum are due entirely to the uncertainties given to the model parameters. The correlation matrix exhibits very strong correlation and anti-correlation coefficients, a signature of model uncertainties as opposed to short-range correlations representative of the influence of experimental uncertainties.

The final evaluated uncertainties are also compared to the recent JENDL-4.0 estimates (see Fig. 29). They lie above those of the JENDL-4.0, but the shapes of the two evaluated curves are very similar and are characteristic of the nature of the spectrum itself (and of the model used to represent it). The lowest uncertainty is obtained near

FIG. 30: Correlation matrix for the $n(0.5 \text{ MeV})+^{238}\text{Pu}$ prompt fission neutron spectrum.

the average outgoing energy, i.e., the first moment of the spectrum.

Last, the average prompt neutron multiplicity $\bar{\nu}_p$ as a function of the incident neutron energy E_{inc} was evaluated at the same time as the corresponding prompt fission spectrum and is shown in Fig. 31 in comparison to the current evaluations of ENDF/B-VII.0, JENDL-4.0 and JEFF-3.1. Experimental data by Jaffey and Lerner [33] and Kroshkin and Zamjatnin [34] exist at the thermal point only. The higher-incident energy points were evaluated through the systematics of Tudora [32], slightly modified to match the experimental data at the thermal energy.

FIG. 31: Average prompt fission neutron multiplicity in the reaction $^{238}\text{Pu}(n,f)$ as a function of the incident neutron energy. Only two experimental data sets exist at the thermal energy point by Jaffey and Lerner [33] and Kroshkin and Zamjatnin [34].

Without additional experimental data more work needs to be done to improve the incident energy dependence of this evaluation.

D. ^{239}Pu

As was the case for $n+^{235,238}\text{U}$ reactions, the uncertainty quantification work for $n+^{239}\text{Pu}$ reaction cross sections was performed for the release of the ENDF/B-VII.0 library, but the evaluated covariance matrices were not included in the library at that time.

The $n+^{239}\text{Pu}$ total cross section, evaluated for ENDF/B-VII.1 (= VII.0), is shown in Fig. 32 in comparison to selected experimental data sets and the JENDL-4.0 and JEFF-3.1 evaluated libraries. Uncertainties were quantified using a statistical analysis of the experimental data sets.

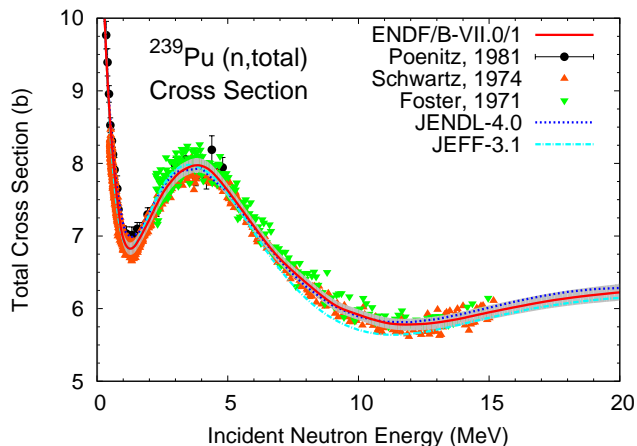


FIG. 32: The ENDF/B-VII.1 (= VII.0) evaluated $n+^{239}\text{Pu}$ total cross-section is shown with a 1σ uncertainty band, and compared to experimental data sets and other evaluated libraries.

The ^{239}Pu (n,f) cross section for ENDF/B-VII.1 (= VII.0) is simply a smoothed version on a finer energy grid of the results from the standards evaluation for ENDF/B-VII.0 [19]. This evaluation with a one-sigma uncertainty band is compared in Fig. 33 with other current evaluations and recent experimental data by Shcherbakov *et al.* [37] and Tovesson *et al.* [38]. Many other data sets were also used in the evaluation.

The ^{239}Pu (n,γ) cross section above the resonance region is taken directly from the ENDF/B-VI.8 evaluation. The result is shown in Fig. 34 with experimental data sets and compared to the JENDL-4.0 and JEFF-3.1 evaluations. All three evaluations and experimental data agree reasonably well below 700 keV, but depart significantly after that. While the evaluated uncertainties below 1 MeV appear reasonable, they may be strongly underestimated above this energy. However, the capture cross section becomes very small in this energy range.

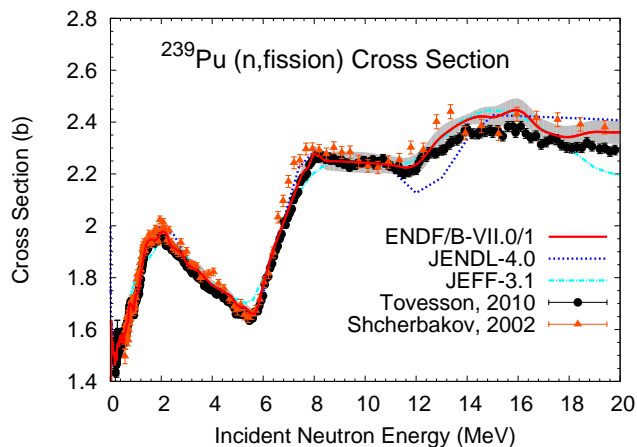


FIG. 33: The neutron-induced fission cross-section of ^{239}Pu evaluated for ENDF/B-VII.0 in the fast energy range is compared to recent measurements by Tovesson *et al.* [38] and Shcherbakov *et al.* [37].

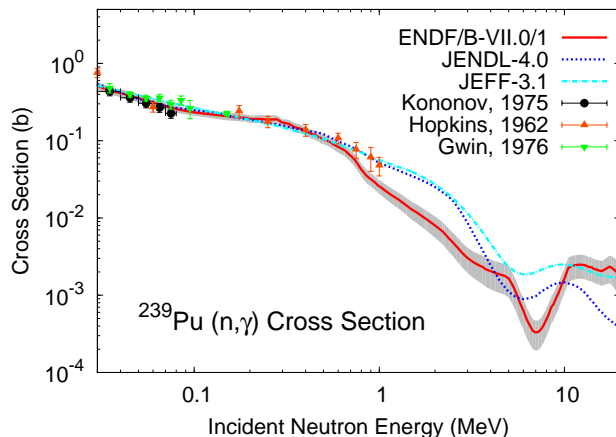


FIG. 34: The ^{239}Pu (n,γ) cross section from 0.03 to 20 MeV shows large discrepancies with other evaluations above 1 MeV, where the capture cross section is then very small.

The total ^{239}Pu (n,n') cross section is shown in Fig. 35 in comparison with experimental data sets from Batchelor *et al.* [39] and Andreev [40], and other current evaluations. This cross section is the sum of low-lying discrete states and continuum cross sections. The low-lying level cross sections are based on coupled-channel model calculations, while direct reaction contributions of high-lying levels were computed in the DWBA formalism.

The evaluation of the ^{239}Pu ($n,2n$) cross section is based largely on a theoretical analysis by McNabb, Chadwick *et al.* using recent experimental data from the LANSCE-GEANIE facility by Bernstein *et al.* [41] and on LLNL data by Lougheed *et al.* [42]. Other experimental data by Mather *et al.* [21] and Frehaut *et al.* [43] were not included in the evaluation due to their large error bars. The result is shown in Fig. 36 with the one-sigma

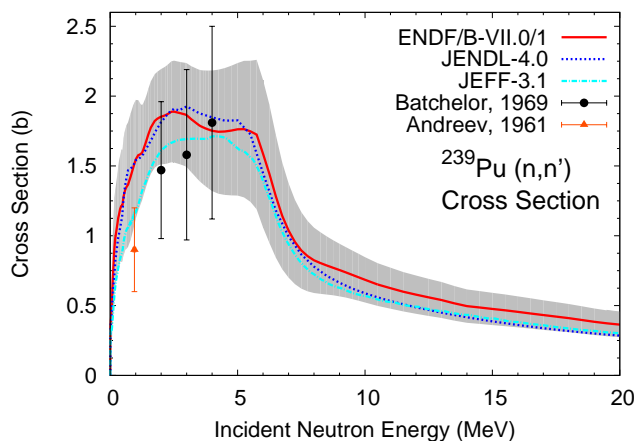


FIG. 35: The ^{239}Pu (n,n') total inelastic cross section is compared to experimental data by Batchelor *et al.* [39] and Andreev *et al.* [40].

uncertainty band. The ENDF/B-VII.1 (= VII.0) evaluation is in good agreement with the JENDL-4.0 values, while the JEFF-3.1 values differ significantly in several places.

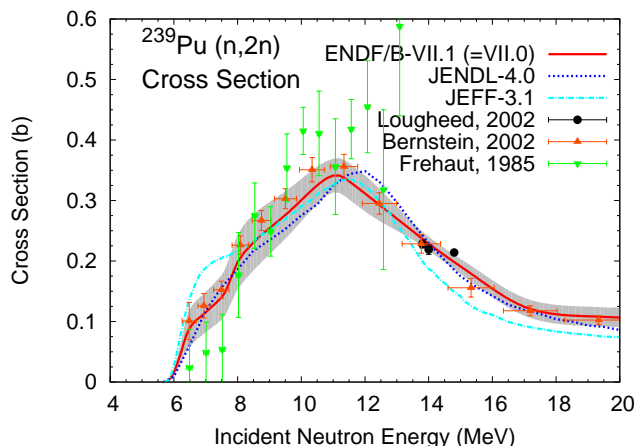


FIG. 36: The ENDF/B-VII.1 (=VII.0) evaluation of ^{239}Pu ($n,2n$) cross section was obtained mostly from recent experimental data by Bernstein *et al.* [41] and LLNL data by Loughheed *et al.* [42].

The evaluated standard deviations for all major reaction cross sections is summarized in Fig. 37.

Uncertainties associated with the prompt fission neutron spectrum of ^{239}Pu (n,f) reaction were not evaluated at the time of the ENDF/B-VII.0 release, but instead were quantified later as an initial attempt to quantify uncertainties of the PFNS for actinides [7]. Following an approach similar to UQ for cross sections, we evaluated a covariance matrix associated with the PFNS for ^{239}Pu induced by 0.5 MeV incident neutrons. A Bayesian inference scheme was used to combine uncertainties stemming from experiments as well as model parameters.

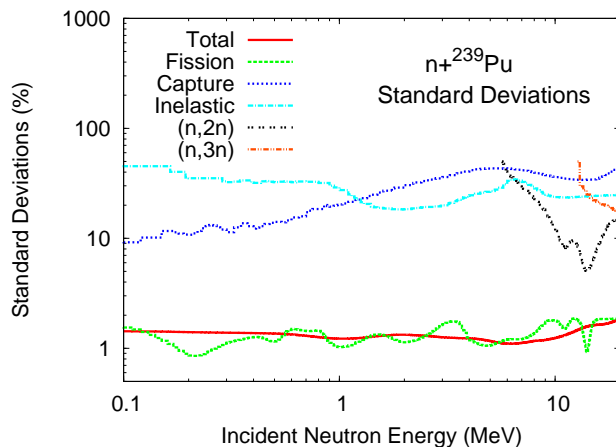


FIG. 37: Standard deviations evaluated for all major reaction channel cross sections for $n+^{239}\text{Pu}$.

Since the ENDF/B-VII.0 PFNS evaluations for all major actinides are based on Madland-Nix model calculations [12], the same model was used in our UQ work. Sensitivity coefficients for model parameters were calculated for the most important parameters. Since we were only concerned with the 0.5 MeV incident neutron energy, only the first-chance fission component contributes, and the relevant parameters are then the average total kinetic energy $\langle TKE \rangle$, the average energy release $\langle E_r \rangle$, the average level density parameter $\langle a \rangle$, and the average neutron separation energy $\langle S_n \rangle$.

The results are shown in Figs. 38, 39 and 40. The error band was increased below 500 keV to take into account observed discrepancies between experimental data sets, and to account for possible limitations of the model to describe the low-energy tail of the spectrum, which is notoriously difficult to measure. The standard deviations as a function of the outgoing neutron energy are shown in Fig. 39 and are in fair agreement with a similar estimate in the JENDL-4.0 library. The correlation matrix is shown in Fig. 40 and is the result of the complete uncertainty quantification procedure, including the ad-hoc corrections below 500 keV. This can be compared to the PFNS correlation matrix for ^{238}Pu (see Fig. 30) for which no experimental data exist.

The average prompt fission neutron multiplicity $\bar{\nu}_p$ as a function of incident neutron energy is shown in Fig. 41, and compared to a subset of experimental data sets and the JENDL-4.0 and JEFF-3.1 evaluations. There is a large scatter of points, and the evaluation is based on a least-square fit of all data sets. The JENDL-4.0 evaluation is based mainly on the data by Gwin *et al.* [44], even following some “fluctuations” around 20 keV. The ENDF/B-VII.0 as well as the JEFF-3.1 evaluations have a smoother behavior in this region. The uncertainty band is the result of the covariance analysis, smoothed out following simple physical considerations.

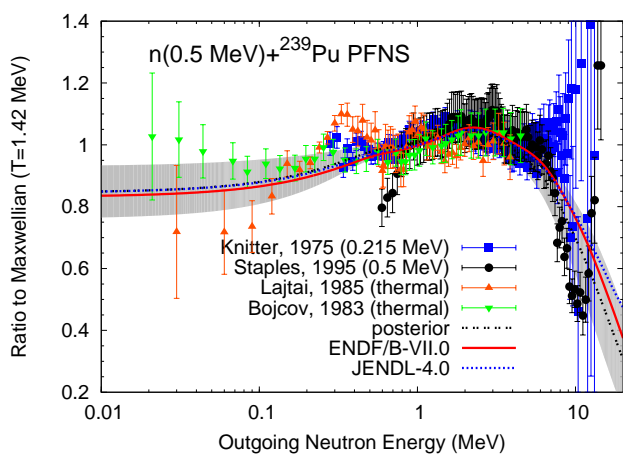


FIG. 38: The ENDF/B-VII.0 evaluated prompt fission neutron spectrum for the $n(0.5 \text{ MeV})+^{239}\text{Pu}$ reaction is shown with experimental data and the JENDL-Actinoid result. The one-sigma uncertainty band was obtained by first reproducing the ENDF/B-VII.0 PFNS result, then by assuming error bands for the Los Alamos model parameters, and including experimental data constraints.

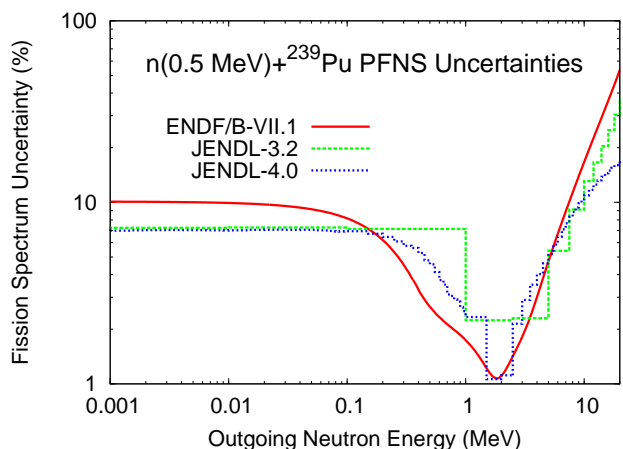


FIG. 39: The calculated standard deviations for the evaluated PFNS of $n(0.5 \text{ MeV})+^{239}\text{Pu}$ is compared to the JENDL-4.0 evaluation.

E. ^{240}Pu

GNASH sensitivity calculations were performed varying the following set of model parameters: $(E_A, E_B, \hbar\omega_A, \hbar\omega_B, \rho_A, \rho_B)$ for the first, second and third compound nuclei formed in the $n+^{240}\text{Pu}$ reaction. These are the fission barrier heights, barrier widths and collective enhancement factors on top of the barriers, respectively. We also varied the level density parameters, pairing energies, pre-equilibrium constants and experimental γ -ray strength function.

A host of experimental data sets was gathered for each reaction channel, as shown in Table II. In addition, a recent measurement of the ^{240}Pu ($n, \text{fission}$) cross section

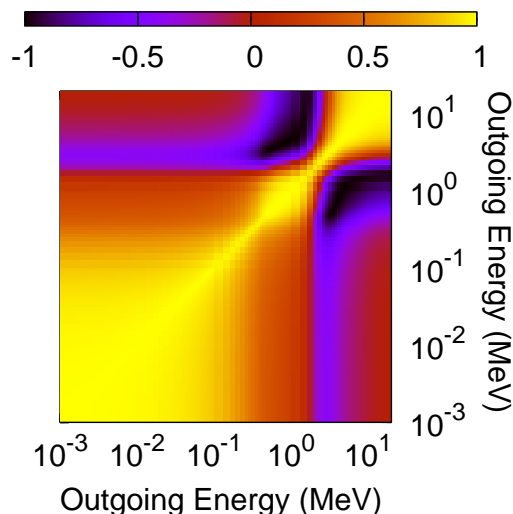


FIG. 40: Correlation matrix evaluated for the $n(0.5 \text{ MeV})+^{239}\text{Pu}$ prompt fission neutron spectrum.

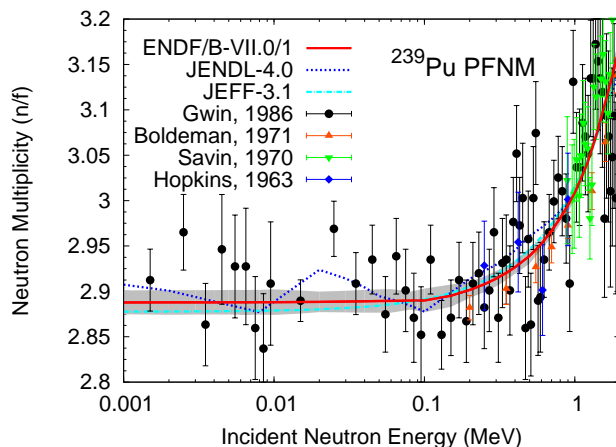


FIG. 41: ^{239}Pu average prompt fission neutron multiplicity as a function of incident neutron energy.

performed at the Los Alamos Neutron Science Center (LANSCE) by Tovesson *et al.* [46] was included in the present analysis.

The ^{240}Pu neutron-induced fission cross section is shown in Fig. 42, and its associated correlation matrix is shown in Fig. 43. All fission cross section measurements were done in ratio to the ^{235}U (n, f) cross section standard. These ratio data sets were transformed into absolute data points using the ENDF/B-VII.0 standard ^{235}U (n, f) cross sections [19]. The large number of these data sets and their reported small uncertainties leads to final evaluated uncertainties for the fission cross section that are quite small. We have added a 0.3% fully-correlated contribution to the final covariance matrix, as has been already done in the case of the ^{235}U fission cross sec-

TABLE II: Experimental cross-section data for $n+^{240}\text{Pu}$ reaction channels. The references are taken directly from the EXFOR database.

Reaction	EXFOR Entry	First Author	Year	Reference
Total	10179-002	A.B. Smith	1972	(J,NSE,47,19,197201)
	10935-009	W..P. Poenitz	1981	(J,NSE,78,333,81)
	12853-057	W.P. Poenitz	1983	(R,ANL-NDM-80,8305)
Capture	10766-002	L.W. Weston	1977	(J,NSE,63,143,77)
	20765-003	K. Wisshak	1978	(J,NSE,66,(3),363,197806)
	20765-004	K. Wisshak	1978	(J,NSE,66,(3),363,197806)
	20767-002	K. Wisshak	1979	(J,NSE,69,(1),39,7901)
Elastic	10179-003	A.B. Smith	1972	(J,NSE,47,19,197201)
	12742-007	A.B. Smith	1982	(C,82ANTWER,,39,8209)
Fission	10597-002	J.W. Behrens	1978	(J,NSE,66,433,197806)
	12714-002	J.W. Meadows	1981	(J,NSE,79,233,8110)
	13576-002	J.W. Behrens	1983	(J,NSE,85,314,8311)
	13801-003	P. Staples	1998	(J,NSE,129,149,1998)
	21764-002	C. Budtz-Jørgensen	1981	(J,NSE,79,4,380,81)
	21764-004	C. Budtz-Jørgensen	1981	(J,NSE,79,4,380,81)
	22211-002	T. Iwasaki	1990	(J,NST,27,(10),885,199010)
	40509-002	V.M. Kupriyanov	1979	(J,AE,46,(1),35,197901)
	41444-002	A.V. Fomichev	2004	(R,RI-262,2004)
	41487-002	A.B. Laptev	2007	(C,2007SANIB,,462,200710)
	14223-002	F. Tovesson	2009	(J,PR/C,79,014613,2009)

tion. Better evaluation tools aimed at better describing correlations (in energies, isotopes, reactions) have to be developed to properly tackle this recurrent problem in current covariance matrix evaluations.

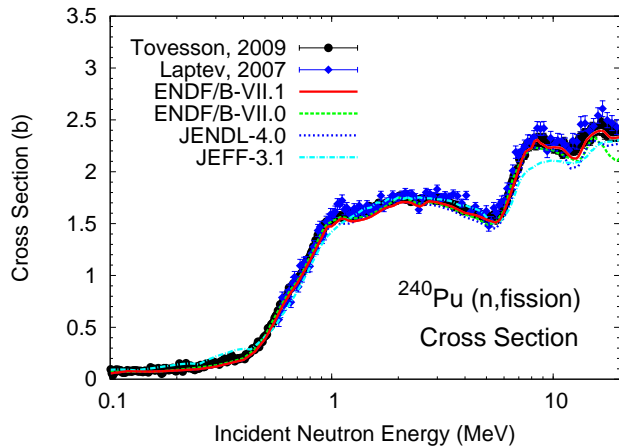


FIG. 42: The evaluated neutron-induced fission cross-section of ^{240}Pu is shown in compared to the two most recent data sets by Tovesson *et al.* [46] and Laptev *et al.* [47].

The ^{240}Pu (n,total) cross section shown in Fig. 44 is also relatively well known, and our optical model calculations using the optical model potential by Soukhovitskii *et al.* [48] could reproduce the experimental data quite well. The correlation matrix for the (n,total) cross section is shown in Fig. 45.

The ^{240}Pu (n,γ) cross section is shown in Fig. 46. Ex-

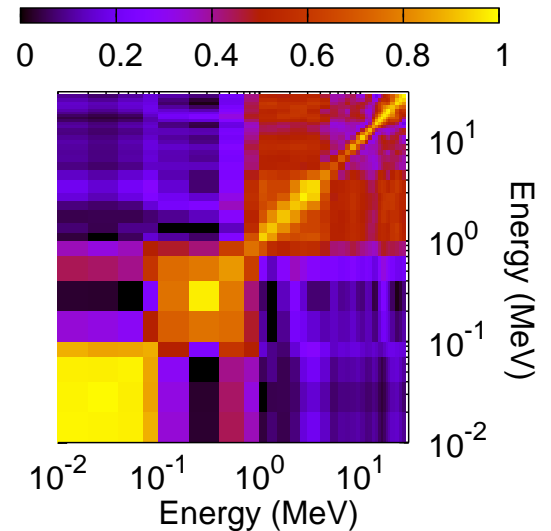


FIG. 43: Evaluated correlation matrix for the neutron-induced fission cross section of ^{240}Pu in the fast energy range.

perimental data sets are in good agreement up to about 300 keV. The lack of experimental data above this energy and the drop in magnitude of the cross sections largely increase the evaluated uncertainties there— a cap uncertainty of 100% was used to avoid numerical problems with the covariance matrix. The correlation matrix for the capture cross section is shown in Fig. 47 and reveals large off-diagonal elements above 100 keV, due mostly to

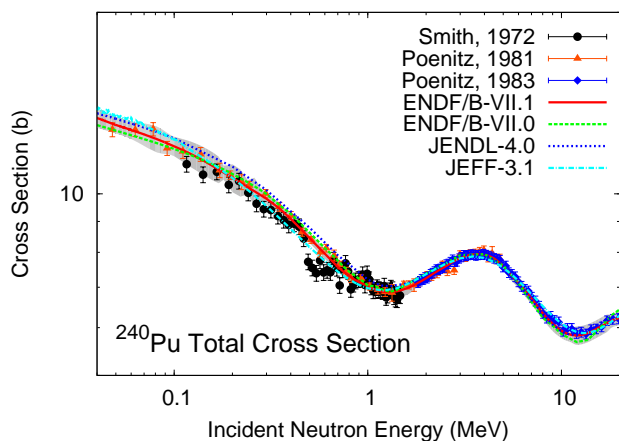


FIG. 44: A covariance analysis was performed on the ^{240}Pu (n,total) cross section experimental data sets. Coupled-channel calculations could reproduce this cross section quite well.

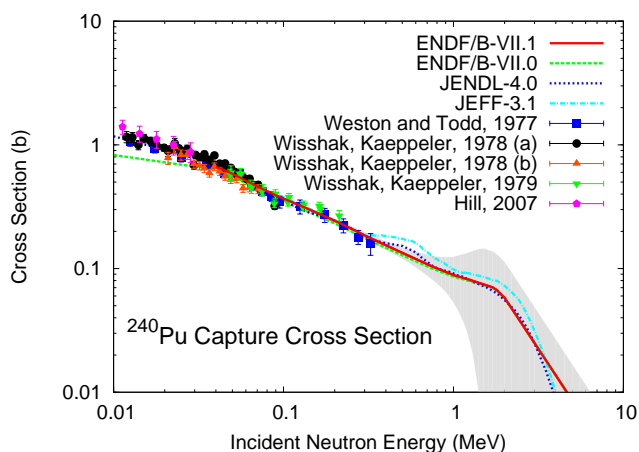


FIG. 46: ^{240}Pu (n, γ) cross-section.

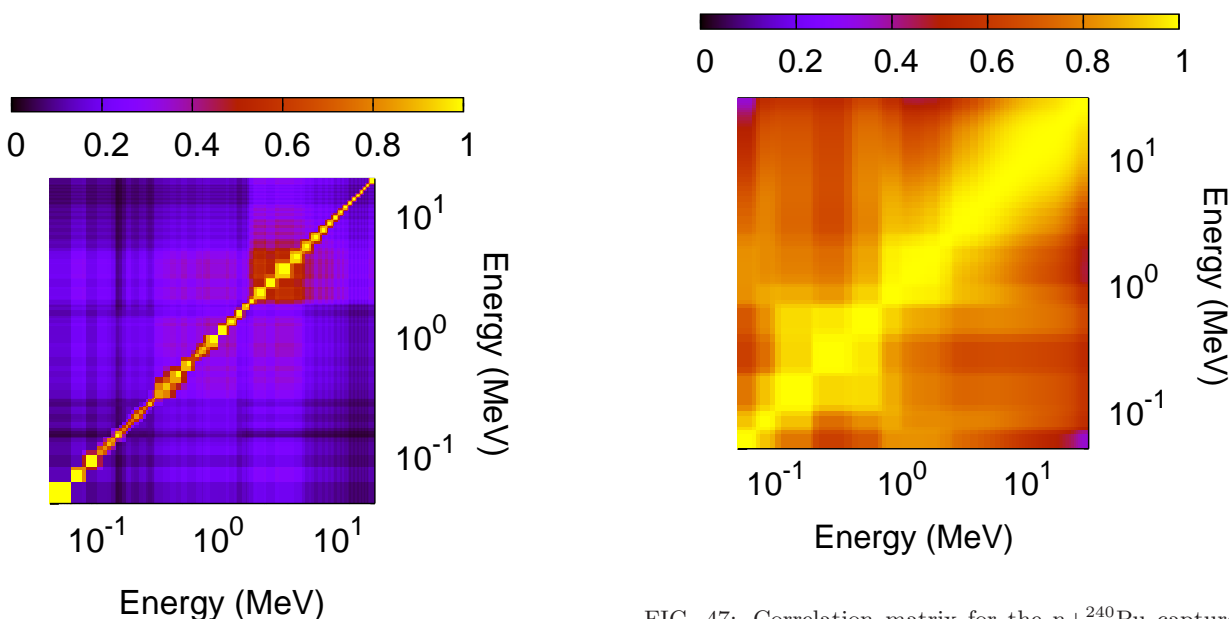


FIG. 45: ^{240}Pu (n,total) cross section correlation matrix.

model parameter uncertainties, and a lack of experimental data in this energy range. The capture cross section standard deviations were re-normalized to 3% around 100 keV- point-wise experimental uncertainties, while the raw KALMAN result gave about 1.5% instead.

Finally, no measurements exist for the inelastic, (n,2n) and (n,3n) cross sections. Therefore our uncertainty estimates, shown in Figs. 48, 49 and 50, for those reactions are based solely on GNASH model sensitivity calculations. Cross-correlations between open reaction channels are important however, and are calculated with the NJOY processing code.

The average prompt fission neutron multiplicity $\bar{\nu}_p$ for $n+^{240}\text{Pu}$ was evaluated through a covariance analysis of

available experimental data sets, and is shown in Fig. 51 with data sets and other current evaluations.

Figure 52 summarizes the results for the standard deviations on all major reaction cross sections for $n+^{240}\text{Pu}$.

F. ^{241}Pu

A new evaluation of neutron-induced reactions on ^{241}Pu is in progress and will eventually be incorporated in later releases of the ENDF/B-VII library. However, at this time, a new covariance matrix evaluation for the neutron-induced fission cross-section only was performed and is included in the VII.1 library. It is based solely

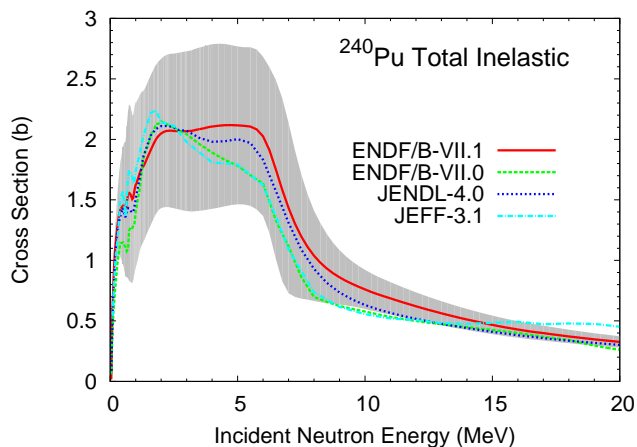


FIG. 48: The ^{240}Pu total inelastic cross section is compared to other current evaluations. No experimental data exist for this cross section.

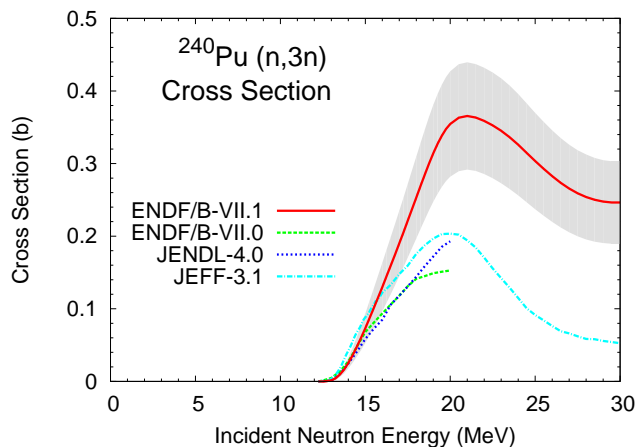


FIG. 50: The ENDF/B-VII.1 evaluated ^{240}Pu (n,3n) cross section is compared to other current evaluations.

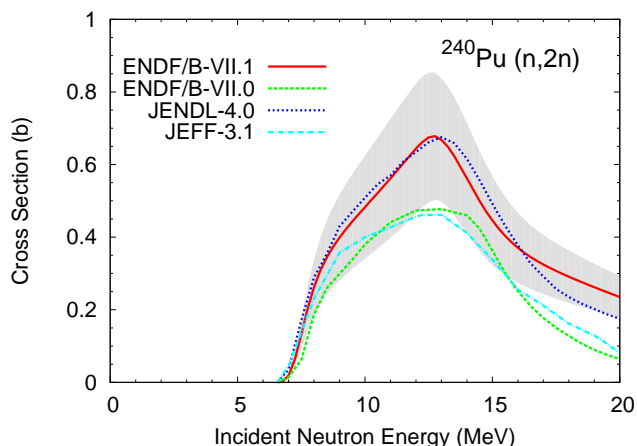


FIG. 49: The ^{240}Pu (n,2n) cross section is compared to other current evaluations. No experimental data exist for this cross section.

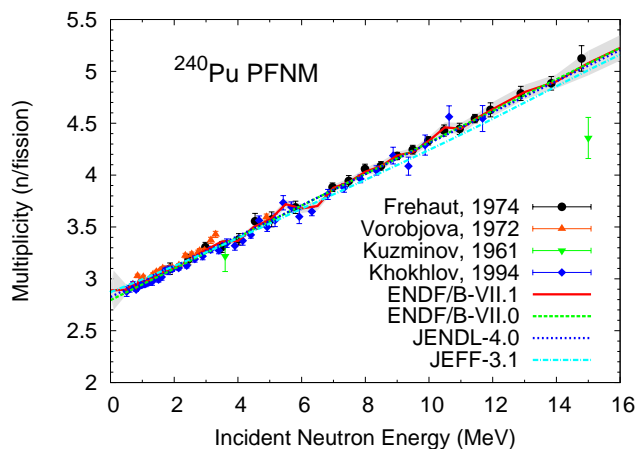


FIG. 51: The ^{240}Pu average prompt fission neutron multiplicity was evaluated through a covariance analysis of the available experimental data sets.

on a statistical analysis of the experimental fission cross-section data using the GLUCS code. A recent experiment by Tovesson and Hill [38] was performed at LANSCE and was included in the present analysis. Most fission data were obtained in ratio to the standard ^{235}U (n,f) cross section, and those data are shown in Fig. 53 along with the ENDF/B-VII.0 data. This figure was obtained by processing the two ENDF/B-VII.1 files for ^{235}U and ^{241}Pu with the NJOY code in a fine 640-group structure, and then taking their ratio.

As can be inferred from this figure, the experimental ratio data are fairly consistent over the energy range considered (10 keV – 20 MeV) except for the recent LANSCE data that deviates from the bulk of the other data points below about 1 MeV. The latter data have been obtained in similar ways as the other plutonium isotopes [38, 46] for which no large deviation from the ENDF/B-VII.0 results was observed. The source of this discrepancy re-

mains largely unknown, so at this stage, we decided to cut off the LANSCE data below 0.9 MeV for our statistical analysis. The reason for this is two-fold: (i) the bulk of the other data sets, albeit much older, are consistent with each other and with a higher ratio value below 1 MeV; (ii) integral feedback [49] from the COSMO critical experiment at MASURCA, Cadarache, show that the ENDF/B-VII.0 evaluated fission cross-section, which follows the higher ratio values, leads to a C/E very close to unity for the ^{241}Pu fission rate (see Table 6 in Ref. [49]). A decrease in the ^{241}Pu (n,f) cross section in the hundreds of keV region would clearly deteriorate this agreement.

G. Other Actinide Evaluations

Additional UQ evaluations were performed for other actinides (e.g., $n+^{233}\text{U}$, $n+^{241}\text{Am}$) that have not been

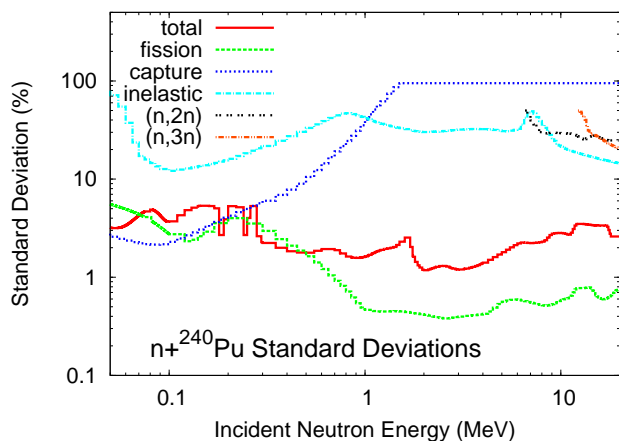


FIG. 52: Standard deviations evaluated for the fission, capture, inelastic, (n,2n) and (n,3n) reaction cross sections of ^{240}Pu .

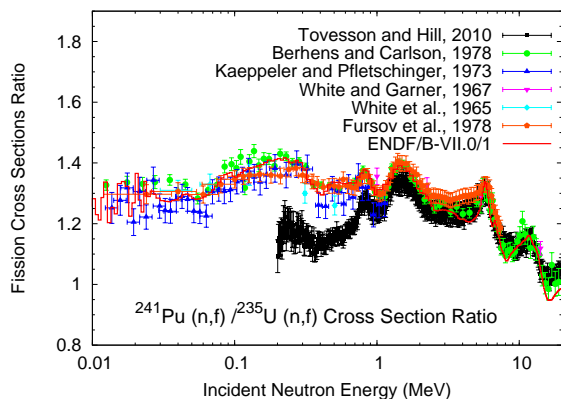


FIG. 53: The ratio of ^{241}Pu (n,f) cross-section to ^{235}U (n,f) cross-section is shown in a 640-group structure, processed with NJOY, for the ENDF/B-VII.0 evaluation, and compared with experimental ratio data. The ^{235}U (n,f) cross section was taken from the evaluated standards [19].

discussed in this paper. However, the methods and tools used were the same as those presented above, and the results can readily be found in the ENDF/B-VII.1 library.

IV. SUMMARY AND OUTLOOK

This paper discusses the quantification of uncertainties associated with new or recent data evaluations of neutron-induced reaction on selected actinides, as performed at LANL in the fast energy range. The methodology used throughout this work is one that tries to assess sources of uncertainties stemming from both experimental data and model parameter uncertainties. In many cases, the evaluation of the nuclear data was performed prior to the quantification of uncertainties, thereby creating a somewhat inconsistent approach. This problem

was minimized by staying close to the data evaluation process, using the same nuclear reaction codes and the same experimental database. Newer evaluations, e.g., for $n+^{238,240}\text{Pu}$, do not present the same intrinsic difficulties.

The result of this work is a large set of covariance matrices for the major reaction cross sections for neutron-induced reactions on the following actinides: $^{233,235,238}\text{U}$, $^{238,239,240,241}\text{Pu}$ and ^{241}Am . In the case of $n+^{241}\text{Pu}$, only the fission cross-section covariance matrix has been evaluated so far, while other channels will be tackled in the near future. In addition, some covariance matrices have been evaluated for the prompt fission neutron spectrum for low-incident neutron energies.

At this stage, we should also note that the covariance matrices evaluated in this work do not strictly follow the ENDF-6 format for MF=33, NC-type, LTY=1 sub-subsections, which specifies that covariances in sub-subsections defined in a narrower energy range than the evaluation itself should be given explicitly as zero outside this smaller range. The NJOY code would assign zero automatically outside the range of the evaluated covariances, but that is not necessarily the case for other processing codes.

While it is clear that this work represents a major evaluation effort and a leap forward in terms of covariance matrices in the ENDF/B-VII library, one should still consider those covariance matrices as a first attempt at assessing uncertainties in evaluated nuclear data files in a scientific-based approach. Much work remains to improve upon those matrices in order to represent the full evaluation process as faithfully as possible. A particular effort should be devoted to a better representation of the experimental uncertainties and of their correlations in and between experiments. While such detailed approach has been used for the standards evaluation, much less has been done for other reactions and isotopes. Important coding efforts will also focus on better integrating the different components of the evaluation process.

The unresolved resonance region represents an interesting challenge where much progress can be made by accounting for the matching between different reaction models where they overlap in this energy range. Such work would lead to correlations between the resolved resonance range and the fast energy range, which are totally absent from the current covariance matrices.

This first generation of covariance matrices is already used successfully in nuclear reactor sensitivity calculations (e.g. Refs. [1, 50]) to study the impact of uncertainties in current nuclear data libraries on reactor integral parameter uncertainties, and to assess where future research efforts, experimental as well as theoretical, should be directed. In particular, deficiencies in evaluated inelastic and capture cross sections, prompt fission neutron spectra and multiplicities are apparent from this work.

Obviously, many other applications, e.g., nuclear medicine, astrophysics, etc, would also benefit significantly from quantified uncertainties associated with evaluated nuclear data.

Acknowledgments

The authors would like to sincerely thank A.D. Carlson and D.L. Smith, as well as the Nuclear Data Sheets

referees, for their insightful remarks and suggestions to improve the first draft of this publication.

-
- [1] M. Herman, P. Obložinský, C.M. Mattoon, M. Pigni, S. Hoblit, S.F. Mughabghab, A. Sonzogni, P. Talou, M.B. Chadwick, G.M. Hale, A.C. Kahler, T. Kawano, R.C. Little, and P.G. Young, “COMMARA-2.0 Neutron Cross Section Covariance Library,” BNL-94830-2011 Technical Report (2011).
- [2] M.B. Chadwick, P. Obložinský, M. Herman, N.M. Greene, R.D. McKnight, D.L. Smith, P.G. Young, R.E. MacFarlane, G.M. Hale, S.C. Frankle, A.C. Kahler, T. Kawano, R.C. Little, D.G. Madland, P. Möller, R.D. Mosteller, P.R. Page, P. Talou, H. Trellue, M.C. White, W.B. Wilson, R. Arcilla, C.L. Dunford, S.F. Mughabghab, B. Pritychenko, D. Rochman, A.A. Sonzogni, C.R. Lubitz, T.H. Trumbull, J.P. Weinman, D.A. Brown, D.E. Cullen, D.P. Heinrichs, D.P. McNabb, H. Derrien, M.E. Dunn, N.M. Larson, L.C. Leal, A.D. Carlson, R.C. Block, J.B. Briggs, E.T. Cheng, H.C. Huria, M.L. Zerkle, K.S. Kozier, A. Courcelle, V. Pronyaev, and S.C. van der Marck, “ENDF/B-VII.0: Next Generation Evaluated Nuclear Data Library for Nuclear Science and Technology,” Nuclear Data Sheets **107**, 2931 (2006).
- [3] M.B. Chadwick, M. Herman, P. Obložinský *et al.*, “ENDF/B-VII.1 Nuclear Data for Science and Technology: Cross Sections, Covariances, Fission Product Yields and Decay Data,” Nuclear Data Sheets **112**, 2887 (2011).
- [4] L. Leal, K. Guber, D. Wiarda, D. Arbanas, H. Derrien, R. Sayer, N.M. Larson, M.E. Dunn, “ORNL Resolved Resonance Covariance Generation for ENDF/B-VII.1,” Nuclear Data Sheets, submitted.
- [5] “Covariance Data in the Fast Neutron Region,” M. Herman, Coordinator, A. Koning, Monitor, OECD, NEA/WPEC-24 (2011).
- [6] Rev. Mr. Bayes, “An Essay towards Solving a Problem in the Doctrine of Chances,” Phil. Trans. **53**, 370 (1763).
- [7] P. Talou, T. Kawano, D.G. Madland, A.C. Kahler, D.K. Parsons, M.C. White, R.C. Little, and M.B. Chadwick, “Uncertainty Quantification of Prompt Fission Neutron Spectrum for $n(0.5 \text{ MeV})+^{239}\text{Pu}$,” Nucl. Sci. Eng. **166**, 254 (2010).
- [8] J. Raynal, “Notes on ECIS94,” Centre d’Études Nucléaires, Saclay, report CEA-N-2772 (1994).
- [9] P. G. Young, E.D. Arthur, and M. B. Chadwick, “Comprehensive Nuclear Model Calculations: Theory and Use of the GNASH Code,” in Proceedings of the Workshop on Nuclear Reaction Data and Nuclear Reactors, ICTP, Trieste, Italy, 15 April - 17 May 1996, Ed: A. Gandini and G. Reffo, World Scientific Publ. Co., Singapore, p.227-404 (1998).
- [10] T. Kawano, P. Talou, M.B. Chadwick, and T. Watanabe, “Monte Carlo Simulation for Particle and Gamma-Ray Emissions in Statistical Hauser-Feshbach Model,” J. Nucl. Sci. Tech. **47**, No. 5, 462 (2010).
- [11] P. Talou, “Prompt Fission Neutron Calculations in the Madland-Nix Model”, P.Talou, LANL Technical Report, LA-UR-07-8168 (2007).
- [12] D. G. Madland and J. R. Nix, “New calculation of prompt fission neutron spectra and average prompt neutron multiplicities”, Nucl. Sci. Eng. **81**, 213 (1982).
- [13] T. Kawano and K. Shibata, “Covariance Evaluation System,” JAERI-Data/Code 97-037 (in Japanese) Technical Report (1997).
- [14] R.E. MacFarlane, “The NJOY Nuclear Data Processing System, Version 91”, Los Alamos National Laboratory Technical Report, LA-1274-M (1994).
- [15] H. Leeb, D. Neudecker, and Th. Srdinko, “Consistent Procedure for Nuclear Data Evaluation Based on Modeling,” Nuclear Data Sheets **109**, Issue 12, 2762 (2008).
- [16] P. Talou, T. Kawano, and P. G. Young, “Covariance matrices for ENDF/B-VII ^{235}U , ^{238}U and ^{239}Pu evaluated files in the fast energy range”, in Proceedings of the International Conference on Nuclear Data for Science and Technology, April 22-27, 2007, Nice, France, editors O. Bersillon, F. Gunsing, E. Bauge, R. Jacqmin, and S. Leray, EDP Sciences, p. 293 (2008).
- [17] P.G. Young and E.D. Arthur, “Theoretical Analyses of (n,xn) Reactions on ^{235}U , ^{238}U , ^{237}Np , and ^{239}Pu for ENDF/B-VI,” Proc. Int. Conf. on *Nuclear Data for Science and Technology*, Julich, Germany, 13-17 May 1991, Ed. S.M. Qaim, Springer-Verlag, p. 894 (1992).
- [18] R. Capote, M. Herman, P. Obložinský, P.G. Young, S. Goriely, T. Belgya, A.V. Ignatyuk, A.J. Koning, S. Hilaire, V.A. Plujko, M. Avrigeanu, O. Bersillon, M.B. Chadwick, T. Fukahori, Zhigang Ge, Yinlu Han, S. Kailas, J. Kopecky, V.M. Maslov, G. Reffo, M. Sin, E.Sh. Soukhovitskii and P. Talou, “RIPL - Reference Input Parameter Library for Calculations of Nuclear Reactions and Nuclear Data Evaluations,” Nuclear Data Sheets **110**, 3107 (2009).
- [19] A.D. Carlson, V.G. Pronyaev, D.L. Smith, N.M. Larson, Zhenpeng Chen, G.M. Hale, F.-J. Hamsch, E.V. Gai, Soo-Youl Oh, S.A. Badikov, T. Kawano, H.M. Hofmann, H. Vonach, and S. Tagesen, “International Evaluation of Neutron Cross Section Standards,” Nuclear Data Sheets **110**, 3215 (2009).
- [20] J. Fréhaut, A. Bertin, and R. Bois, “Measurement of the ^{235}U (n,2n) Cross Section between Threshold and 13 MeV”, Nucl. Sci. Eng. **74**, 29 (1980).
- [21] D.S. Mather, P.F. Bampton, R.E. Coles, G. James, and N.J. Nind, “Measurement of (n,2n) Cross Sections for Incident Energies between 6 and 14 MeV,” Aldermaston Report AWRE-O-72/72 (1972).
- [22] F.H. Fröhner, Nucl. Sci. Eng. **103** (1988); F.H. Fröhner, Proc. Int. Conf. on Reactor Phys., Jackson Hole, Wyoming (1988) Vol. III, p. 171.
- [23] W.P. Poenitz, L.R. Fawcett Jr., and D.L. Smith, Nucl. Sci. Eng. **78**, 239 (1981).
- [24] Y. Kanda and M. Baba, “WPEC-SG4 Report: ^{238}U Capture and Related Cross Sections,” Tech. Rep. WPEC/SG4, NEA, Paris (1999).

- [25] D. Drake, I. Bergqvist, and D.K. McDaniels, "Dependence of 14 MeV Radiative Neutron Capture on Mass Number," *Phys. Lett. B* **36**, 557 (1971).
- [26] D.K. McDaniels, P. Varghese, D.M. Drake, E. Arthur, A. Lindholm, I. Bergqvist, J. Krumlinde, "Radiative Capture of Fast Neutrons by ^{165}Ho and ^{238}U ," *Nucl. Phys. A* **384**, 88 (1982).
- [27] L.R. Veaser and E.D. Arthur, "Measurement of (n,3n) Cross Sections for U-235 and U-238," *Proc. Int. Conf. on Neutron Physics and Nuclear Data for Reactors and Other Applied Purposes*, AERE Harwell, U.K., 25-29 Sep. 1978, p. 1054.
- [28] J. Frehaut, Nuclear Energy Agency Nuclear Data Committee Report NEANDC(E) 238/L (1986).
- [29] J. Taieb, T. Granier, T. Ethvignot, M. Devlin, R.C. Haight, R.O. Nelson, J.M. O'Donnell, and D. Rochman, "Measurement of the Average Energy and Multiplicity of Prompt Fission Neutrons from ^{238}U (n,f) and ^{237}Np (n,f) from 1 to 200 MeV," *Proc. Int. Conf. on Nuclear Data for Science and Technology*, Nice, France, April 2007, Vol.1, p.429 (2007).
- [30] G.S. Boykov, V.D. Dmitriev, G.A. Kudyaev, Yu.B. Ostapenko, M.I. Svirin, and G.N. Smirenkin, "Neutron Spectrum in the Fission of ^{232}Th , ^{235}U and ^{238}U by Neutron with Energies 2.9 and 14.7 MeV," *Yad. Fiz.* **53** (3), 628 (1991).
- [31] M. G. Silbert and J. R. Berreth, "Neutron Capture Cross Section of Plutonium-238: Determination of Resonance Parameters," *Nucl. Sci. Eng.* **52**, 187 (1973).
- [32] A. Tudora, "Systematic Behaviour of the Average Parameters Required for the Los Alamos Model of Prompt Neutron Emission," *Annals of Nuclear Energy* **36**, 72 (2009).
- [33] A.H. Jaffey and J.L. Lerner, "Measurement of Prompt Neutron Fission Yield in Thermal Neutron Fission of U-232, Pu-238, Pu-241, Am-241, Am-242m, Cm-243, Cm-245 and in Spontaneous Fission of Cm-244," *Nucl. Phys. A* **145**, 1 (1970).
- [34] N.I. Kroshkin and J.S. Zamjatnin, "The Measurement of Energy Spectra and Average Number of Prompt Fission Neutrons $\bar{\nu}$," *Atomic Energy* **29**, 95 (1970).
- [35] J.J. Ressler, J.T. Burke, J.E. Escher, C.T. Angell, M.S. Basunia, C.W. Bausang, L.A. Bernstein, D.L. Bleuel, B.L. Goldblum, J. Gostic, R. Hatarik, R.A. Henderson, J. Munson, E.B. Norman, L.W. Phair, T. Ross, N.D. Scielzo, M. Wiedeking, "Surrogate Measurement of the ^{238}Pu (n,f) Cross Section", LLNL Technical Report LLNL-TR-457798 (2010).
- [36] T. Granier, R. Nelson, P. Romain, M. Devlin, and N. Fotiades, "New Measurement of the ^{238}Pu (n,f) Cross-Section", in *Proceedings of the Fourth International Workshop on Nuclear Fission and Fission-Product Spectroscopy*, Cadarache, France, 13-16 May 2009, Eds. A.Chatillon, H.Faust, G.Fioni, D.Goutte, H.Goutte, AIP CP1175, p.227 (2009).
- [37] O.A. Shcherbakov, A.Yu. Donets, A.V. Evdokimov, A.V. Fomichev, T. Fukahori, A. Hasegawa, A.B. Laptev, V.M. Maslov, G.A. Petrov, Yu.V. Tuboltsev, and A.S. Vorobiev, "Neutron-Induced Fission of U-233, U-238, Th-232, Pu-239, Np-237, nat-Pb and Bi-209 Relative to U-235 in the Energy Range 1-200 MeV", *J. Nucl. Science and Technology*, Tokyo, Supplement, Vol.2, Issue 1, p.230 (2002).
- [38] F. Tovesson and T. S.Hill, "Cross Sections for ^{239}Pu (n,f) and ^{241}Pu (n,f) in the range $E_n=0.01$ eV to 200 MeV," *Nucl. Sci. Eng.* **165**, 224 (2010).
- [39] R. Batchelor and K. Wyld, "Neutron Scattering by ^{235}U and ^{239}Pu for Incident Neutrons of 2, 3 and 4 MeV," Report AWRE-O-55/69 (1969).
- [40] V.N. Andreev, "Inelastic Scattering of Neutrons of the Fission Spectrum and Neutrons with an Energy of 0.9 MeV in U2 and Pu239," *Nejtronfiz* **287** (1961).
- [41] L.A. Bernstein, J.A. Becker, P.E. Garrett, W. Younes, D.P. McNabb, D.E. Archer, C.A. McGrath, H. Chen, W.E. Ormand, M.A. Stoyer, R.O. Nelson, M.B. Chadwick, G.D. Johns, W.W. Wilburn, M. Devlin, D.M. Drake, and P.G. Young, " ^{239}Pu (n,2n) ^{238}Pu Cross Section Deduced Using a Combination of Experiment and Theory," *Phys. Rev. C* **65**, 021601 (2002).
- [42] R.W. Loughheed, W. Webster, M.N. Namboodiri, D.R. Nethaway, K.J. Moody, J.H. Landrum, R.W. Hoff, R.J. Dupzyk, J.H. McQuaid, R. Gunnink, E.D. Watkins, " ^{239}Pu and ^{241}Am (n,2n) Cross-Section Measurements Near $E_n = 14$ MeV," *Radiochim. Acta*, **90**, 833 (2002).
- [43] J. Frehaut, A. Bertin, R. Blois, E. Gryntakis, and C.A. Philis, "(n,2n) Cross Sections of 2-H and 239-Pu," *Proc. Int. Conf. on Basic and Applied Science*, Santa Fe, NM, 1985, p. IB06 (1985).
- [44] R. Gwin, R.R. Spencer, and R.W. Ingle, "Measurements of the Energy Dependence of Prompt Neutron Emission from ^{233}U , ^{235}U and ^{239}Pu for $E_n=0.0005$ to 10 MeV Relative to Emission from Spontaneous Fission of ^{252}Cf ," *Nucl. Sci. Eng.* **94**, 365 (1986).
- [45] T. E. Young, F. B. Simpson, J. R. Berreth, and M. S. Coops, "Neutron total and absorption cross sections of ^{238}Pu ," *Nucl. Sci. Eng.* **30**, 355 (1967).
- [46] F. Tovesson, T. S. Hill, M. Mocko, J. D. Baker, and C. A. McGrath, "Neutron induced fission of ^{240}Pu and ^{242}Pu from 1eV to 200 MeV", *Phys. Rev. C* **79**, 014613 (2009).
- [47] A.V. Laptev, A.Yu. Donets, V.N. Dushin, A.V. Fomichev, A.A. Fomichev, R.C. Haight, O.A. Shcherbakov, S.M. Soloviev, Yu.V. Tuboltsev, and A.S. Vorobyev, "Neutron-Induced Fission Cross Sections of ^{240}Pu , ^{243}Am , and ^{nat}W in the Energy Range 1-200 MeV", *Proc. Int. Conf. on Nuclear Data for Science and Technology*, ND2004, Sep.26-Oct.1, 2004, Santa Fe, USA, AIP CP769, Eds. R.C. Haight, M.B. Chadwick, T. Kawano, and P. Talou, p.865 (2004).
- [48] E. Soukhovitskii, S. Chiba, J.-Y. Lee, O. Iwamoto, T. Fukahori, "Global coupled-channel optical potential for nucleon-actinide interaction from 1 keV to 200 MeV", *Journal Phys. G: Nucl. Part. Phys.* **30**, 905 (2004).
- [49] G. Palmiotti, M. Salvatores, G. Aliberti, H. Hiruta, R. McKnight, P. Obložinský, and W. S. Yang, "A Global Approach to the Physics Validation of Simulation Codes for Future Nuclear Systems," *Annals of Nuclear Energy* **36**, 355 (2009).
- [50] G. Aliberti, G. Palmiotti, M. Salvatores, T.K. Kim, T.A. Taiwo, M. Anitescu, I. Kodeli, E. Sartori, J.C. Bosq, and J. Tommasi, "Nuclear Data Sensitivity, Uncertainty and Target Accuracy Assessment for Future Nuclear Systems," *Annals of Nuclear Energy* **33**, 700 (2006).